1963

Instability of cylindrical reactor fuel elements

Benjamin Mingli Ma
Iowa State University

INSTABILITY OF CYLINDRICAL REACTOR FUEL ELEMENTS

by

Benjamin Mingli Ma

A Dissertation Submitted to the
Graduate Faculty in Partial Fulfillment of
The Requirements for the Degree of
DOCTOR OF PHILOSOPHY

Major Subject: Nuclear Engineering

Approved:

Signature was redacted for privacy.

In Charge of Major Work

Signature was redacted for privacy.

Head of Major Department

Signature was redacted for privacy.

Dean of Graduate College

Iowa State University
Of Science and Technology
Ames, Iowa

1963

TABLE OF CONTENTS

NOTATION

a_0, a, b, c_0, c = constants

C_1, C_2, $\cdots$, C_6 = integration constants

d = extrapolated distance

D_1, D_2 = diffusion coefficients, D_0 = diffusion coefficient in fuel

E_f = energy released per fission

f(t) = function of time or irradiation time

$f_1(x)$, $f_2(x)$ = functions of x

$F(\sigma)$, $F_1(\sigma)$ = functions of effective stress

g(T) = function of temperature or irradiation temperature

$g_1(x)$, $g_2(x)$ = functions of x

G_i, G_t = irradiation and thermal-cycling growth coefficients

g_1, g_2 = constants

G, H, J, G_1, G_2 = constants

h, h_i, h_0 = thickness of inner and outer cladding

$H(\epsilon)$ = function of effective strain

$I_0(\varkappa_i r_i)$, $I_1(\varkappa_i r_i)$, $I_2(\varkappa_i r_i)$ = modified Bessel functions of the first kind of the ith order, i = 0, 1, 2

$K_0(\varkappa_i r_i)$, $K_1(\varkappa_i r_i)$, $K_2(\varkappa_i r_i)$ = modified Bessel functions of the second kind of the ith order, i = 0, 1, 2

J_1, J_2, J_3 = first, second and third stress invariants for fuel material

J_{2_c} = second stress invariant for cladding material

k = thermal conductivity of fuel material

ℓ, ℓ' = actual and extrapolated lengths of fuel element

L_0, L = initial and final lengths of fuel specimen

M_1, M_2, M_3, M_4 = constants

N = number of atoms or number of cycles, n = neutron density

p = strain parameter

q_1, q_2 = slowing-down densities of neutrons in moderators

q_v = volumetric heat generation rate

Q = total rate of heat generation or heat transfer per unit length of fuel element

Q_{r_i}, Q_{r_0} = Q at r_i and r_0

$Q_T = Q_{r_i} + Q_{r_0}$

Q_{av} = average rate of heat generation or heat transfer per unit length of fuel element

Q_{max} = maximum rate of heat generation or heat transfer per unit length of fuel element

r = radius

r_i, r_0, r_m = inner, outer and mean radii of fuel zone

r_1 = outer radius of the moderator

$(r)_{\theta_{max}}$ = radius at θ_{max} in fuel

$s = \frac{1}{2}(\sigma_r - \sigma_t)$

s_r, s_t, s_z = radial, tangential and axial components of deviatoric stress for fuel material

s_{r_c}, s_{t_c}, s_{z_c} = radial, tangential and axial components of deviatoric stress for cladding material

STP = standard temperature and pressure

T_0 = initial or ambient temperature

T = temperature or irradiation temperature

u_r = radial displacement of cylindrical surface for fuel material

$\dot{u}_r$ = time rate of change in radial displacement

$u = u_r/r_0$, $\dot{u} = \dot{u}_r/r_0$, $u_0 = u$ at r_0

$x = r/r_0$, $x_i = r_i/r_0$, $x_m = r_m/r_0$

z, z' = axial coordinates of fuel element

$f(z)$, $f(z')$ = functions of z and z'

α, α_c = linear coefficients of thermal expansion for fuel and cladding materials

β = fraction of total heat transferred by inner passage of coolant

ϕ = neutron flux or thermal neutron flux at r_0

ϕ_0 = thermal neutron flux in fuel

ϕ_1, ϕ_2 = thermal neutron flux in moderators

Σ_{a_0} = macroscopic absorption cross section of fuel

Σ_{a_1}, Σ_{a_2} = macroscopic absorption cross sections of moderators

Σ_f = macroscopic fission cross section of fuel

κ_0, κ_1, κ_2 = reciprocal diffusion lengths

∇^2 = Laplacian operator

$\theta = T - T_0$ = effective temperature

θ_{r_i}, θ_{r_0} = effective temperatures at r_i and r_0

θ_{max} = maximum effective temperature

θ_c, θ_{c_i}, θ_{c_0} = effective temperatures of cladding at r_i and r_0

$\dot{\theta}$ = time rate of change of effective temperature

$\epsilon = \frac{1}{2}(\epsilon_r - \epsilon_t)$ = effective creep strain

ϵ_r, ϵ_t, ϵ_z = radial, tangential and axial strains of fuel

ϵ_{r_i}, ϵ_{t_i}, ϵ_{z_i}, ϵ_{r_o}, ϵ_{t_o}, ϵ_{z_o} = radial, tangential and axial strains of fuel at r_i and r_o

ϵ_{r_c}, ϵ_{t_c}, ϵ_{z_c} = radial, tangential and axial strains of cladding

ϵ_R = resultant linear thermal and radiation dilatation

ϵ_I = linear thermal-cycling and radiation dilatation

ϵ_{I_o} = linear thermal-cycling and radiation dilatation at x_m

$\dot{\epsilon}$, $\dot{\epsilon}_r$, $\dot{\epsilon}_t$, $\dot{\epsilon}_z$, $\dot{\epsilon}_R$, $\dot{\epsilon}_I$ = time rates of change of ϵ, ϵ_r, ϵ_t, ϵ_z, ϵ_R and ϵ_I respectively

σ_{ij} = stress tensor

σ = effective stress

$\bar{\sigma}$ = mean normal stress

σ_r, σ_t, σ_z = radial, tangential and axial components of creep stress

σ_{r_i}, σ_{t_i}, σ_{z_i}, σ_{r_o}, σ_{t_o}, σ_{z_o} = σ_r, σ_t, σ_z at r_i and r_o of fuel

$(\sigma_{r_i})_c$, $(\sigma_{t_i})_c$, $(\sigma_{z_i})_c$ = σ_{r_i}, σ_{t_i}, σ_{z_i} at r_i of cladding

λ = parameter

μ = irradiation hardening coefficient

ψ = angle

$\psi(\sigma,T,t)$ = function of σ, T and t

$\psi_1(\sigma,\epsilon,T)$ = function of σ, T and ϵ

$\Psi(\sigma,t,T)$ = function of σ, T and t

ρ = density of uranium fuel

I. INTRODUCTION

A. Importance of Stability of the Fuel Elements in Power Reactors

The fuel element is the central and most significant single component in the heterogeneous reactor systems. The study of stability of the fuel element in high power reactors is of scientific and technological importance. The origin of instability occurring in fuel elements is primarily the thermal and radiation effects, namely, thermal-cycling growth, irradiation growth and swelling of nuclear fuel materials. Some severe thermal and radiation effects on the fuel material can produce appreciable creep strains and stresses which, in turn, bring about the physical and mechanical instability of the fuel element.

In general, uranium as well as plutonium fuel exhibits high plasticity and accelerated creep under irradiation and burn-up in a high integrated neutron flux. This property of radiation damage is more pronounced in U^{235} enriched fuel.

As a matter of fact, the successful operation, performance and economics of a nuclear power reactor depend, to a large extent, upon the physical and mechanical integrity of the fuel elements. In other words, the successful operation, performance and economics of a large nuclear power plant

depend chiefly on the adequate physical and mechanical stability of the fuel elements under irradiation in a high integrated neutron flux.

Further, in order to obtain high thermal efficiency and low costs in a nuclear power plant, the fuel element is usually required to be designed for high surface temperatures and burn-ups. For instance, the fuel element limitations of low surface temperature and burn-up which result in low power output and require short re-fuel cycles, will increase the operation and fuel costs. However, apart from the irradiation and thermal effects, the higher are the desirable surface temperature and burn-up, the greater the physical and mechanical instability of the fuel elements will be.

Therefore, the radiation damage, thermal effect and the required higher surface temperature and burn-up of the fuel material pose an important scientific and technological problem in the development of a fuel element which has the physical and mechanical stability for a successful operation, performance and economics of a nuclear power reactor.

B. The Categories of the Reactor Fuel Elements

According to the physical and chemical properties of the fissionable materials, the fuel elements used for nuclear reactors can be divided into the following two main categories:

1. Metallic fuel elements
2. Ceramic (compounds of metallic and non-metallic elements) fuel elements

More elaborately, according to the compositions of the fuel material, the fuel elements may be further classified as

1. Massive uranium metal fuel elements
2. Uranium alloy fuel elements
3. Uranium-compound dispersion fuel elements

The massive uranium metal fuel elements are mainly used in the reactors for plutonium production such as Oak Ridge Graphite Reactor, X-10. Because of their relatively low initial cost such fuel elements can also be used for power reactors as the graphite-moderated and gas-cooled Calder Hall type reactors. Massive uranium can be operated to have almost zero irradiation and thermal-cycling growths by making the grain size fine and the crystal orientation random. This is usually done by suitable beta-quenching or powder metallurgy method. These metallurgical treatments are effective, however, only if the metal fuel elements are operated in a reactor with maximum core temperatures that do not exceed the alpha-beta transformation temperature. Since uranium exists in three allotropic forms of the lattice cell,

(a) Alpha uranium (orthorhombic), below 662° C
(b) Beta uranium (tetragonal), between 662 and 770° C
(c) Gamma uranium (BCC), from 770° C to melting point

1130° C.

Therefore, the maximum core temperature in a reactor operation must be below 662° C when massive uranium metal fuel elements are used.

Uranium alloy fuel elements developed also exist as the gamma-phase alloy fuel elements because a few alloying elements added to uranium tend to retain and stabilize the gamma phase appreciably (1). Among the alloying elements which produce expanded gamma-phase regions in the binary uranium systems are Nb, Zr, Ti, Mo and V. The first three of these are completely soluble in the gamma-phase uranium at elevated temperatures while the last two provide extended gamma-phase regions with limited solubilities. The gamma-phase alloy fuel elements have shown great promise of achieving high resistance to irradiation growth and swelling and great corrosion resistance to water at elevated temperatures. For example, the Mo gamma-phase alloy fuel elements have been selected and are in use for the Enrico Fermi Power Reactor (2). Although zirconium alloy fuel elements have better aqueous corrosion resistance and nuclear properties (relatively small thermal and epithermal neutron absorption cross sections) than the molybdenum alloy fuel elements, the physical and mechanical stability of the latter is considerably greater than the former under high flux irradiation. Therefore, in this particular case in developing and selecting a suitable fuel

element for the power reactor, the physical and mechanical stability was still the primary consideration.

The uranium-compound dispersion fuel elements refer, in common, to those in which uranium compounds (especially UO_2, $UO_2 \cdot ThO_2$) with enriched U^{235} is contained in metallic cladding or dispersed in metal matrix. For example, fuel elements with UO_2 of high enrichment dispersed in aluminum base have been in process or in use for the MTR (Material Testing Reactor) type research reactors and for the Borax-V type power reactors (3).

Recently, considerable interest has centered around dispersion type fuel elements because the need for greater thermal efficiency and lower operation cost in the production of nuclear power demands the development of such fuel elements that can operate at high temperatures, high burn-ups and great resistance to aqueous corrosion. The dispersion type fuel elements is one of the promising ways to meet these requirements above.

The dispersion type fuel elements possess two unique advantages over solid homogeneous elements (4):

(a) Long service life because of localization of fission-product damage

(b) More choice of fuel-element structures or claddings.

The proper selection of fissile and nonfissile materials to be used in a dispersion type fuel element involves the con-

sideration of various factors. Of primary concern are compatibility of the fissile and nonfissile phases at both fabricating and operating temperatures, the neutron absorption cross sections of fuel and matrix, density of the uranium compound, weight percentage of uranium in the fissile phase and corrosion resistance of the nonfissile phase.

The ideal dispersion fuel element incorporates the fissile and nonfissile materials without any metallurgical reaction and, consequently, retains the desirable properties of the matrix material that provides the structural strength to the fuel element. Therefore, the fissile material should contain relatively high content of uranium, maintain size and shape during fabrication and operation and be insensitive to radiation damage at higher burn-ups. Likewise the matrix material should be strong, ductile and insensitive to radiation damage either.

For fabrication of dispersion fuel elements, the powder metallurgy is far superior to melting or casting method.

From the foregoing discussion it is seen that for low burn-ups and low core temperatures operated below the alpha-beta transformation temperature, the massive uranium metal fuel elements can be used to the advantages:

(a) Low initial fuel cost

(b) Plutonium production

while for high burn-ups and high core temperatures operated

above the alpha-beta transformation temperature, either the gamma-phase alloy or the uranium-compound dispersion fuel elements can be utilized. Both have high radiation stability and aqueous corrosion resistance.

C. Advantages and Disadvantages of Metallic and Ceramic Fuel Elements

Both metallic and ceramic fuel elements have certain advantages and disadvantages. In general, the advantages of the metallic fuel elements are

1. High uranium atom density
2. Good thermal conductivity for heat transfer and utilization
3. Fairly large ductility

In contrast, the advantages of the ceramic fuel elements are

1. Great heating-resistance and very high melting point which compensate for very poor thermal conductivity
2. High aqueous corrosion resistance
3. Relatively low irradiation growth and swelling

Evidently, an extensive comparison between the physical, chemical and mechanical properties of metals and ceramics will reveal that the advantages of the metallic fuel elements are just the disadvantages of the ceramic fuel elements, and vice versa.

It can be concluded from the above that the uranium alloy and the uranium-compound dispersion fuel elements are respectively the improved, promising metallic and ceramic fuel elements.

Although the ceramic fuel elements have recently gained ground, the inherent advantages of the metallic fuel elements still hold basic incentives. Because with a given power rating for a power reactor, these inherent advantages of the metallic fuel elements directly affect the reactor size. The ceramic fuel elements require a substantially larger fuel lattice which may result in more difficult design problems for both the fuel elements and the entire reactor. Therefore, there still are the basic incentives to develop simple, compact uranium alloy fuel elements for power reactors that can operate at high temperatures, high burn-ups and great resistance to various corrosion conditions.

II. RADIATION AND THERMAL EFFECTS ON URANIUM FUELS

A. Introduction to Radiation and Thermal Effects

The primary radiation and thermal effects on uranium fuels directly in connection with the stability of fuel elements used for nuclear power reactors are

1. Irradiation growth and swelling
2. Surface wrinkling, cracking, porosity and hardness
3. Thermal-cycling growth

These effects pose some serious scientific and technological problems in the development of economical nuclear power therein the stability of the fuel elements is of great importance.

B. Irradiation Growth and Swelling

The phenomena of irradiation growth and swelling in both metallic uranium and ceramic fuels resulting from radiation damage are basically different in nature. The irradiation growth is the dimensional instability due to the basic anisotropy of uranium, while the irradiation swelling is the volumetric instability caused by the inert gases of fission products in the fuel. If the differentiation between irradiation growth and irradiation swelling is made on the basis of fuel density, we may define that irradiation growth is a

change in shape with a minor change in density, while irradiation swelling is a change in volume with a major decrease in density. In addition, irradiation growth generally occurs at relatively low temperatures, less than about 350° C, while irradiation swelling is generally associated with temperatures appreciably higher than 350° C (5). The threshold temperature for initiation of swelling has not been determined. It may range from 450° C to 650° C.

Experimental data obtained from irradiated single crystals of alpha uranium show that the crystal lattice elongates in the (010) direction, contracts in the (100) direction and the (001) direction remains unchanged in length (6). This proves the facts that

(a) The irradiation growth of anisotropic deformation is merely a change in shape.

(b) The irreversible ratchet and the anisotropic diffusion mechanisms proposed to interpret the irradiation growth are, by large, applicable (7).

A single crystal after irradiation and careful measurements may give the three lattice growth coefficient, G_i, in microunits of growth per length for one fission per million total atoms, N. Based on the known exponential relationship between initial and final lengths, L_o and L, of the specimen, the growth coefficient can be expressed as

$$G_i = \frac{1}{L}\frac{dL}{dN} = \frac{\ln (L/L_o)}{\text{fraction of total atoms fissioned}} \qquad (2.1)$$

This exponential relationship will be used in connection with creep analysis for stress distribution in the fuel elements later.

Since the length changes in the specimen are small, Eq. 2.1 may be approximated as

$$G_i = \frac{\% \text{ length change}}{\% \text{ atoms burn-up}} \qquad (2.2)$$

Experiments in which fuel specimens have been taken to high burn-up have shown that in some cases G_i may vary with burn-up. The growth coefficient, however, falls to zero in the neighborhood of 450° C (8), i.e., the growth rate vanishes in the region of 450° C.

There is no evidence of any basic difference between growth of single crystals under irradiation and growth of polycrystalline aggregates so that each individual crystal in the aggregates will tend to elongate in the (010) direction and contract in the (100) direction, but will be, more or less, constrained by its neighboring grains. The effect of such constraint is obviously greater for fuel materials which have fine grains and random grain orientation, as mentioned in Section IB, so that the irradiation growth may be minimized.

In general, the irradiation growth of the fuel materials

depends not only on the temperature, change in lengths, grain size and orientation but also on the chemical composition of the fuel. Under the same conditions, the irradiation growth produced in the ceramic fuel is usually less than that in the metallic one (4). As shown in Eq. 2.1, the irradiation growth of uranium fuels can be represented by an exponential function of burn-up, which depends on total integrated flux, ϕt (=nvt), where ϕ is the neutron flux and t is the time. The higher is the neutron flux, the higher is also the burn-up and irradiation temperature.

The irradiation swelling in uranium fuels results from a number of separate mechanisms, the relative importance of which varies according to the irradiation temperature. Three possible mechanisms have been observed in volume increase (8):

1. Increase in volume of fissioned atoms

   Of all the fission products are taken into account, one fissioned uranium atom replaced by two atoms of greater average size will result in a volume increase of about 3% for 1% burn-up.

2. Low temperature distortion

   The distortion and intergranular stresses in uranium due to irradiation growth at low temperatures cause micro-structure tears which result in volume increase.

3. The separation of the fission product gases, such as xenon and krypton, into gas bubbles at higher temperatures,

where automatic diffusion is possible, swelling occurs on the separation of these inert gases into bubbles. One per cent of burn-up produces about five times the atomic volume of the gases at STP. A severe decrease in the uranium density tends to increase the volume with increasing temperature and burn-up.

To sum up, among the above mechanisms, the first is not serious, the second and third occur in different temperature ranges. The most important one in magnitude is the third.

It is seen from above that the chief cause of the irradiation swelling is the production of atoms of the inert gases by fission products and is most severe at higher temperatures.

Realistically, there is a continual desire for higher operating temperatures and higher burn-ups in power reactors which, in turn, increase the production of the inert gases and irradiation swelling. Therefore, the irradiation swelling and the stability of the fuel elements used for power reactors become one of the most important problems in the development of economical nuclear power.

In order to lessen and minimize the effect of irradiation swelling, recently the uranium alloy gamma-phase fuel elements and the uranium-compound dispersion fuel elements have been advanced, as already discussed in Section IB.

C. Surface Wrinkling, Cracking, Porosity and Hardness

The surface wrinkling or roughening of uranium is consequence of the identical mechanisms that cause irradiation growth in uranium fuel given above.

Irradiation frequently produces cracking in uranium. This is the result of fracture of radiation-embrittled crystal structures under intergranular and thermal stresses. The origin of the internal cracks before expansion may be the agglomeration of the fission-product gases which also cause the irradiation swelling.

Porosity is serious when uranium fuel is operated at higher temperatures and higher burn-ups. This is consequence of the same mechanisms that produce the irradiation swelling.

Metallic uranium fuel under irradiation became increasingly hard and brittle with continued exposure. The causes of the increased hardness and brittleness are apparently the fission products formed in the fuel. In the creep analysis for stress distribution in the fuel element the effect of the irradiation or strain hardening will be taken into consideration.

D. Thermal-Cycling Growth

Operating temperature in a nuclear reactor is neither homogeneous nor stationary. Kinetics of the reactor results in thermal transients or cycles throughout the systems. Apart from start-up and shutdown of the reactor where highly transient state exists, the instantaneous neutron flux will also produce thermal cycling to the fuel elements in the reactor core.

Experimentally, substantial dimensional and structural changes in polycrystalline uranium fuel have been observed when the fuel was subjected to repeated heating and cooling in the alpha-phase temperature range (from room temperature to 662° C (9, 10). In cast fuel, the dimensional changes manifest themselves in the form of surface roughening, in wrought fuel, the dimensional changes take the form of substantial elongations, generally in directions coincident with the direction of mechanical work. This phenomenon is known as thermal-cycling growth, corresponding to irradiation growth of the uranium fuel.

The extent of the dimensional and structural changes is a function of the number of cycles to which the material is submitted. The thermal-cycling growth depends on a number of variables that may be divided into two main categories:

1. Material variables

2. Cycling variables

Among the material variables, the most important are

a. Grain size

b. Preferred grain orientation

c. Chemical composition

Among the cycling variables, the most important are

a. Temperature limits of the cycle

b. Cycling range

c. Rate of repeated heating and cooling

d. Holding time at each temperature limit

Similar to Eq. 2.1 for the irradiation growth, the three lattice growth coefficient, G_t, produced by the thermal cycling in alpha uranium can be given by

$$G_t = \frac{1}{L}\frac{dL}{dN} = \frac{\ln (L/L_o)}{\text{Fraction of total number of cycles}} \qquad (2.3)$$

in which L_o = initial length of the specimen

L = the length of the specimen after N cycles

N = number of cycles

When $\ln (L/L_o)$ is plotted versus N, the plot is usually a straight line (10). In such a case, the growth coefficient, G_t, is simply equal to the slope of the line.

In order to compare the effects of the irradiation growth and the thermal-cycling growth on uranium, the similarities and dissimilarities between these two processes are listed

below.

Similarities

1. Both irradiation and thermal-cycling growths produce extensive changes in shape and dimensional instability of uranium fuels.
2. Both produce growth in the (010) direction and contraction in the (100) direction.
3. Maximum growth produced in each case depends on the maximum (010) preferred grain orientation being in the (010) axis.
4. The anisotropy of the alpha-phase crystal structure is the necessary condition for each process.
5. Microstructural evidence of mechanical strains within the grains and at the grain boundaries exists in each process.
6. In examining the change in crystal structures, the X-ray diffraction lines are broadened in both cases.
7. Fine grain size and random grain orientation may minimize both irradiation and thermal-cycling growths.

Dissimilarities

1. Irradiation growth occurs in single crystals as well as polycrystalline aggregates of uranium, while thermal-cycling growth does not operate with single crystals. The thermal-cycling growth requires true grain boundaries. (A pseudo crystal thermally cycles 769

times between 100 and 500° C did not grow)(11).

2. Irradiation growth embrittles uranium, while thermal-cycling growth does not.
3. Irradiation growth ceases, $G_i = 0$, above about 450° C and is greatest at lower temperature range, 100 - 200° C. Irradiation growth also slows down as temperatures approach absolute zero. Thermal-cycling growth increases rapidly when the upper temperature is raised, and cycling to upper temperature less than 350° C is insensitive.
4. Microstructures of uranium often show profuse twins and slips after irradiation growth, with little sign of polygonization. In contrast, microstructures of thermal cycling exhibit more polygonization but little twinning.
5. The porosity produced in irradiated uranium is attributed to the bubbles of inert gases of fission products, while microstructural porosity in cycled uranium is mechanical in origin.
6. The irradiation growth coefficient, G_i, is a function of burn-up, while the thermal-cycling growth coefficient, G_t, is a function of the number of cycles.

As mentioned for the irradiation growth in uranium, the irreversible ratchet and the anisotropic diffusion mechanisms can also be applied to the phenomenon of thermal cycling (10).

Further, a creep mechanism for continued elongation produced by the thermal cycling may be proposed. When some cycling temperatures are changed on a specimen of polycrystalline uranium, intergranular stresses will result from the incompatible thermal expansions and the inherently basic anisotropy of the crystal structure. The intergranular stresses will bring about those weaker grains of the polycrystalline aggregates to the point of yielding and, subsequently, form the plastic deformation. As the upper cycling temperatures are increased, the stronger grains of the polycrystalline aggregates also become yielding. Finally, from the redistribution of the intergranular stresses among the grains involved in the further incompatible thermal expansions, the continued plastic elongation or the phenomenon of creep will prevail through the process of thermal cycling.

In conclusion, thermal cycling growth is manifest in the form of substantial dimensional and structural changes in the uranium fuel. The extent of the growth is a function of the number of cycles to which the fuel is subjected and, in general, the growth is dependent mainly on the material variables and the cycling variables listed above. That the intergranular stresses and strains result from the anisotropic and incompatible thermal expansions may progress in the following stages:

a. Thermal cycling first reduces the creep strength of

the crystals.

b. Continued thermal cycling brings those weaker grains to the point of yielding and then to that of plastic flow.

c. Finally, all the grains become yielding and plastic flow. Thus the phenomenon of creep prevails.

III. THERMAL AND IRRADIATION CREEP

A. Introduction to the Thermal and Irradiation Creep

In a usual sense, creep may be defined as a slow, continuous and plastic deformation of a solid material under constant load as time increases. The creep produced by thermal effect only is known as the thermal creep. Similarly, the creep produced by irradiation only may be called the radiation or irradiation creep. The effects of the thermal and irradiation creep on the stability of fuel elements used in nuclear power reactors are of great importance.

B. Thermal Creep

Recently, considerable efforts have been given and great progress has been made toward a thorough understanding of the behavior of thermal creep developed in the materials of nuclear power reactors as well as of aerospace vehicles. In fact, the primary importance of the thermal creep in the reactors is the design of the control rods and fuel elements. As discussed in the preceding section, for alpha uranium the creep produced by thermal cycling is one of the dynamic types of the thermal creep which relates to the fundamental interest in the

fuel element design.

C. Irradiation Creep

The fact that creep of alpha uranium is accelerated by irradiation is of great interest both experimentally (12) and theoretically (13). Actually, a great acceleration of the creep rate under irradiation, compared to that without irradiation, has been practically observed. This is contrary to a common sense that uranium under irradiation might reduce the creep rate because the irradiated materials become harder and brittler.

Experimental data obtained from uranium specimens show that:

1. The period of transitory creep for uranium specimens under irradiation is 10-30 hr. while for unirradiated specimens is 200-400 hr. between the primary and secondary stages of creep.
2. The creep rate for specimens with disoriented crystal structure is about 50 times as great as that for the same specimens without irradiation.
3. The difference in creep rates between fine-grained quenched metal and coarse-grained cast metal is reduced from a factor of 5-10 for unirradiated metal to a factor of 1.5-3 for irradiated one.

4. The accelerated creep rate is increased by a factor of 1.5-2.0 at relatively low and high stresses during irradiation.
5. The creep rate of cast metal, as a function of the relative intensity of neutron flux, increases almost linearly with the total integrated neutron flux, nvt, as defined before.
6. The creep rate as well as the irradiation growth rate of UO_2, based on linear analysis of the amount of porosity present after very high burn-up, is considerably less than that of uranium metal (4).

These test results confirm the theoretical prediction that the accelerated creep rate occurring in metallic uranium (as well as ceramic fuels) is a consequence of the phenomenon of irradiation growth (13). In extent, that the creep rate of metallic and ceramic uranium fuels is, more or less, accelerated by irradiation is directly associated with irradiation growth and swelling.

The main reasons or mechanisms from which the creep rate of metallic and ceramic uranium fuels is accelerated under irradiation may be given below:

1. For random polycrystalline metal in the absence of external forces, the basic anisotropy of the crystal structure and variously oriented irradiation-growth strains that occur in each individual grain will produce intergranular

stresses accordingly.

2. In the polycrystalline aggregates, some grains are weak and some are strong. The occurrence of overall creep in the specimen produced by irradiation would require some weaker grains to deform plastically. The threshold intensity of irradiation that causes creep will probably depend on the grain size and orientation in the aggregates.
3. The intergranular stresses and strains produced by the irradiation growth which changes the shape of the specimen anisotropically will eventually decrease the creep strength.
4. Similarly, the intergranular stresses and strains induced by the irradiation swelling that changes the volume of the specimen due to the production of bubbles from the fission-product gases will also promote plastic strains and creep rate.
5. There is a possibility that the release of fission energy locally may, in addition, increase plastic strains and creep rate by imposing great local stresses on the grains around the fission site. For instance, the occurrence of thermal or displacement spikes in an irradiated solid is the evidence of such radiation damage due to local fission-energy release.
6. Irradiation may further accelerate the creep rate of uranium fuel significantly by promoting diffusion of the

fission products at relatively high temperatures.

D. Effects of the Thermal and Irradiation Creep on the Stability of Fuel Elements

As already pointed out, the thermal and irradiation creep bears direct effects on the stability of the fuel elements in the development of economical nuclear power. A successful operation, performance and economics of a nuclear power reactor will depend, to a large extent, on how to control and minimize the thermal and irradiation creep so that the stability of the fuel element used in the reactor can be secured.

Finally, it is possible that there is interaction between thermal and irradiation creep. This may depend on what degree of the interrelations existing between the thermal-cycling growth, irradiation growth and irradiation swelling of the fuel elements.

IV. THERMAL NEUTRON FLUX DISTRIBUTION IN AN INTERNALLY AND EXTERNALLY COOLED CYLINDRICAL FUEL ELEMENT

A. The Basic Neutron Diffusion Equations

An internally and externally cooled cylindrical fuel element in the lattice cell of a heterogeneous reactor is now considered. Dimensionally, the mean radius of the fuel element is much greater than its thickness, and, in turn, the length of the fuel element is much greater than its mean radius. Inside and outside of the fuel element are coolant and moderators of the unit equivalent or lattice cell as shown in Fig. 1. For simplicity, the effect of very thin cladding has been neglected.

To deal with the distribution of thermal neutron flux, ϕ, in the fuel element, the following main assumptions are made:

1. The elementary diffusion theory is applicable.
2. The production of thermal neutrons is uniform in the moderator and is zero in the fuel.

The assumption 1 is accurate if

a. The dimensions of the system are large in comparison to the scattering mean free path of the neutrons.
b. The coolant and moderator of the system do not absorb neutrons very heavily.
c. There is no external neutron source in the system.

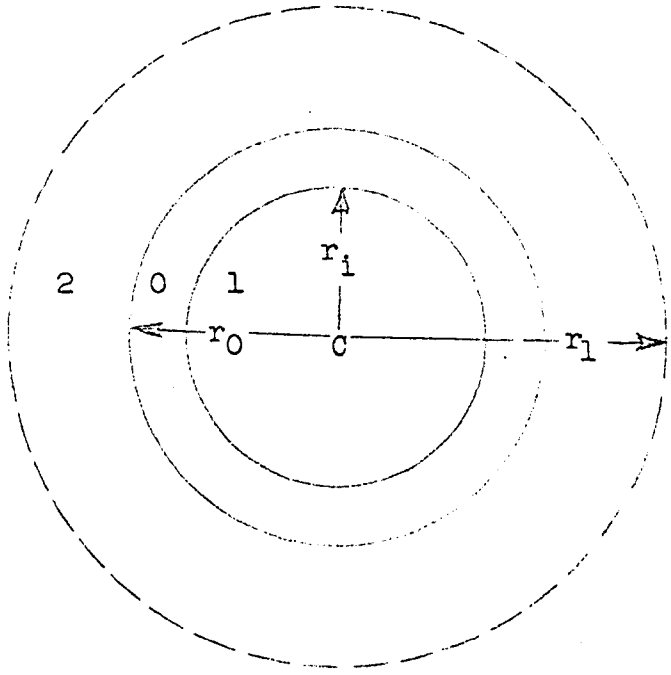

Fig. 1. The fuel element in the lattice cell

r_i = inner radius of the fuel

r_0 = outer radius of the fuel

r_1 = outer radius of the moderator

1 : coolant and moderator

0 : fuel

2 : coolant and moderator

The assumption 2 is valid if

a. The lattice cell size is not large compared to the slowing-down distance of the neutrons.

b. Effects of the all-thermal neutron distribution are cylindrically symmetric (one group model).

On the basis of these assumptions and from the conservation of the neutrons, the diffusion equations in steady state for fuel, moderators as well as coolant are, respectively, given by

$$D_0 \nabla^2 \phi_0 - \Sigma_{a_0} \phi_0 = 0 \qquad \text{in fuel} \qquad (4.1)$$

$$D_1 \nabla^2 \phi_1 - \Sigma_{a_1} \phi_1 + q_1 = 0 \qquad \text{in moderator 1} \qquad (4.2)$$

$$D_2 \nabla^2 \phi_2 - \Sigma_{a_2} \phi_2 + q_2 = 0 \qquad \text{in moderator 2} \qquad (4.3)$$

where

D_0 = diffusion coefficient of the fuel

D_1, D_2 = diffusion coefficients of moderators 1 and 2 respectively

ϕ_0 = neutron flux in the fuel

ϕ_1, ϕ_2 = neutron fluxes in moderators 1 and 2 respectively

Σ_{a_0} = macroscopic absorption cross section of the fuel

Σ_{a_1}, Σ_{a_2} = macroscopic absorption cross sections of moderators 1 and 2 respectively

q_1, q_2 = slowing-down densities of thermal neutrons in moderators 1 and 2 respectively

∇^2 = Laplace's operator

Eqs. 4.1, 4.2 and 4.3 can also be written as

$$\nabla^2\phi_0 - \kappa_0^2\phi_0 = 0 \qquad (4.1a)$$

$$\nabla^2\phi_1 - \kappa_1^2\phi_0 + q_1/D_1 = 0 \qquad (4.2a)$$

$$\nabla^2\phi_2 - \kappa_2^2\phi_2 + q_2/D_2 = 0 \qquad (4.3a)$$

in which

$$\kappa_0^2 \equiv \Sigma_{a_0}/D_0 \ , \qquad \kappa_1^2 \equiv \Sigma_{a_1}/D_1 \ ,$$

$$\kappa_2^2 \equiv \Sigma_{a_2}/D_2$$

κ_0, κ_1, κ_2 are known as the reciprocal diffusion lengths of thermal neutrons in the fuel and moderators respectively.

It may be noted that expression in the form of Eq. 4.1a is often referred to as the wave equation because it is analogous to the equation of wave propagation.

B. The Solutions for Neutron Flux Distribution

For the lattice cell in the cylindrical coordinates, Eqs. 4.1a, 4.2a and 4.3a become

$$\frac{d^2\phi_0}{dr^2} + \frac{1}{r}\frac{d\phi_0}{dr} - \kappa_0^2\phi_0 = 0 \qquad r_i \le r \le r_0 \qquad (4.1b)$$

$$\frac{d^2\phi_1}{dr^2} + \frac{1}{r}\frac{d\phi_1}{dr} - \kappa_1^2\phi_1 + q_1/D_1 = 0 \qquad 0 \le r \le r_i \qquad (4.2b)$$

$$\frac{d^2\phi_2}{dr^2} + \frac{1}{r}\frac{d\phi_2}{dr} - \kappa_2^2\phi_2 + q_2/D_2 = 0 \qquad r_0 \le r \le r_1 \qquad (4.3b)$$

where, by symmetry, the distribution of the thermal neutron flux (one group model) is a function of radius r only.

The general solutions for these equations are given by (see Appendix A)

$$\phi_0 = C_1 I_0(\kappa_0 r) + C_2 K_0(\kappa_0 r) \qquad r_i \le r \le r_0 \qquad (a)$$

$$\phi_1 = C_3 I_0(\kappa_1 r) + C_4 K_0(\kappa_1 r) + q_1/\Sigma_{a_1} \qquad 0 \le r \le r_i \qquad (b)$$

$$\phi_2 = C_5 I_0(\kappa_2 r) + C_6 K_0(\kappa_2 r) + q_2/\Sigma_{a_2} \qquad r_0 \le r \le r_1 \qquad (c)$$

in which

$I_0(\kappa_0 r)$, $I_0(\kappa_1 r)$, $I_0(\kappa_2 r)$ ≡ the modified Bessel functions of the first kind of the zero order

$K_0(\kappa_0 r)$, $K_0(\kappa_1 r)$, $K_0(\kappa_2 r)$ ≡ the modified Bessel functions of the second kind of the zero order

$C_1, C_2, \cdots, C_6$ = integration constants

The boundary conditions of the problem are

ϕ_0 = finite value for r = 0 (d)

$$\phi_0 = \phi_1 \qquad \text{at } r = r_i \qquad (e)$$

$$\phi_0 = \phi_2 \qquad \text{at } r = r_0 \qquad (f)$$

$$D_0\phi_0' = D_1\phi_1' \qquad \text{at } r = r_i \qquad (g)$$

$$D_0\phi_0' = D_2\phi_2' \qquad \text{at } r = r_0 \qquad (h)$$

$$\phi_2' = 0 \qquad \text{for } r = r_1 \qquad (i)$$

By substituting these conditions into (a), (b) and (c), the solutions for the neutron flux distribution are obtained after the integration constants $C_1, C_2, \cdots, C_6$ have been determined. Hence

$$\phi_1 = C_3 I_0(\varkappa_1 r) + q_1/\Sigma_{a_1} \qquad 0 \le r \le r_i \qquad (4.4)$$

$$\phi_2 = \frac{C_6}{I_1(\varkappa_2 r_1)}\left[K_1(\varkappa_2 r_1) I_1(\varkappa_2 r) + I_1(\varkappa_2 r_1) K_0(\varkappa_2 r) \right] + \frac{q_2}{\Sigma_{a_2}}$$

$$r_0 \le r \le r_1 \qquad (4.5)$$

$$\phi_0 = G\,\frac{q_1}{\Sigma_{a_1}} I_0(\varkappa_0 r) - C_2\left[H I_0(\varkappa_0 r) - K_0(\varkappa_0 r) \right]$$

$$r_i \le r \le r_0 \qquad (4.6)$$

where

$$C_2 = \frac{G\left[I_0(\varkappa_0 r_0) - I_1(\varkappa_0 r_0) J \right] + q_2/\Sigma_{a_2}}{H\left[I_0(\varkappa_0 r_0) - I_1(\varkappa_0 r_0) J \right] - \left[K_0(\varkappa_0 r_0 + K_1(\varkappa_0 r_0) J \right]}$$

$$C_3 = D_0\varkappa_0\left[C_1 I_1(\varkappa_0 r_i) - C_2 K_1(\varkappa_0 r_i)\right]/D_1\varkappa_1 I_1(\varkappa_1 r_i)$$

$$C_1 = G\,\frac{q_1}{\Sigma_{a_1}} - C_2 H$$

$$C_6 = \frac{D_0\varkappa_0}{D_2\varkappa_2}\,\frac{\left[GI_1(\varkappa_0 r_0) - C_2\{HI_1(\varkappa_0 r_0) + K_1(\varkappa_0 r_0)\}\right]I_1(\varkappa_2 r_1)}{K_1(\varkappa_2 r_1)I_0(\varkappa_2 r_0) - I_1(\varkappa_2 r_1)K_1(\varkappa_2 r_0)}$$

$$G = I_1(\varkappa_0 r_i)/\left[I_0(\varkappa_0 r_i)I_1(\varkappa_1 r_i)(1 - D_0\varkappa_0/D_1\varkappa_1)\right]$$

$$H = \frac{I_1(\varkappa_0 r_i)K_0(\varkappa_0 r_i) + D_0\varkappa_0 I_0(\varkappa_1 r_i)K_1(\varkappa_0 r_i)/D_1\varkappa_1}{I_0(\varkappa_0 r_i)I_1(\varkappa_1 r_i) - D_0\varkappa_0 I_0(\varkappa_0 r_i)I_0(\varkappa_1 r_i)/D_1\varkappa_1}$$

$$J = \frac{D_0\varkappa_0}{D_1\varkappa_1}\,\frac{K_1(\varkappa_2 r_1)I_0(\varkappa_2 r_0) + I_1(\varkappa_2 r_1)K_0(\varkappa_2 r_0)}{K_1(\varkappa_2 r_1)I_0(\varkappa_2 r_0) - I_1(\varkappa_2 r_1)K_1(\varkappa_2 r_0)}$$

In cases, the fuel element is only externally or internally cooled and moderated, the diffusion equations given above will be automatically reduced from three to two, and the solution of the problem will be greatly simplified. Take, for example, the solid, externally cooled and moderated fuel element. The distribution of thermal neutron flux in the fuel and moderator can be simply given by the relations (16).

$$\phi_0 = \frac{G_1 q_2}{G_2\Sigma_{a_2}} I_0(\varkappa_0 r) \qquad (r_i = 0) \qquad 0 \le r \le r_0 \qquad (4.7)$$

$$\phi_2 = \frac{q_2}{\Sigma_{a_2}}\left[1 + \frac{I_0(\varkappa_2 r)K_1(\varkappa_2 r_1) + K_0(\varkappa_2 r)I_1(\varkappa_2 r_1)}{G_2}\right] \qquad (4.8)$$

$$r_0 < r < r_1$$

in which

$$G_1 = \frac{D_2\varkappa_2}{D_0\varkappa_0}\,\frac{I_1(\varkappa_2 r_0)K_1(\varkappa_2 r_1) - K_1(\varkappa_2 r_0)I_1(\varkappa_2 r_1)}{I_0(\varkappa_0 r_0)}$$

$$G_2 = G_1 I_0(\varkappa_0 r_0) - I_0(\varkappa_2 r_0)K_1(\varkappa_2 r_1) - K_0(\varkappa_2 r_0)I_1(\varkappa_2 r_1)$$

V. HEAT GENERATION DEVELOPED FROM NEUTRON FLUX IN THE FUEL ELEMENT

The rate of heat generation per unit volume, q_v, produced from the neutron flux or energy release from fissions in the fuel can be expressed as

$$q_v = \Sigma_f \phi E_f \quad \text{Mev/cm}^3\text{-sec} \tag{5.1}$$

where

Σ_f = macroscopic fission cross section of the fuel, in cm^{-1}

ϕ = neutron flux, in neutrons/cm^2-sec

E_f = energy released per fission, in Mev/fission

It is well known that the total energy released or available per fission is about 200 Mev or $3.2(10^{-11})$ watt-sec (200 Mev x 1.60 x 10^{-13} watt-sec/Mev).

For a given fissionable material Σ_f is a constant. It is clear from Eq. 5.1 that the rate of heat generation is directly proportional to the neutron flux in the fuel.

Now, introducing Eq. 4.6 given in the preceding section into Eq. 5.1, the rate of heat generation per unit volume of the fuel becomes

$$q_v = \frac{q_1}{\Sigma_{a_1}} \left[g_1 I_0(\varkappa_0 r) + g_2 K_0(\varkappa_0 r) \right] \tag{5.2}$$

in which

$$g_1 = \Sigma_f E_f (G - C_2 H \frac{\Sigma_{a_1}}{q_1})$$

$$g_2 = \Sigma_f E_f C_2 \frac{\Sigma_{a_1}}{q_1} \qquad (5.3)$$

The values of the constants, C_2, G, and H, are, respectively, given in the preceding section.

Here a small fraction of the heat generation rate produced in the coolant and moderators has been neglected, compared to that produced in the fuel.

It may be also noted that the units, Mev per cubic cm per sec, used for the rate of heat generation in Eq. 5.1 are physical units. In heat transfer, however, the practical, engineering units, Btu per cubic ft per hr for the rate of heat generation are commonly used. In order to convert the physical units into engineering units, a convenient conversion factor

$$1 \frac{\text{Mev}}{\text{cm}^3\text{-sec}} \times 1.52\ (10^{-16}) \frac{\text{Btu}}{\text{Mev}} \times 3600 \frac{\text{sec}}{\text{hr}} \times 2.83\ (10^4) \frac{\text{cm}^3}{\text{ft}^3}$$

$$= 1.55\ (10^{-8})\ \text{Btu/ft}^3\text{-hr} \qquad (a)$$

can be used.

In a power reactor design, an average or a maximum rate of heat generation or removal from each fuel element is usually assumed. In order to estimate the average and maximum rate of heat generation. The heat balance for the fuel

element, as shown in Fig. 2 is considered. Let

ℓ = half-length of active zone of the fuel element

$\ell' = \ell + d$ = extrapolated half-length of the fuel element

d = end extrapolation distance for thermal neutron flux

Q_T = total heat-generation rate per unit length of the fuel element

Q_{av} = average total heat generation rate per unit length of the fuel element

Q_{max} = maximum total heat generation rate per unit length of the fuel element

$f(z)$ = distribution function for axial heat generation of the fuel element

$f(z')$ = extrapolated function for axial heat generation of the fuel element

For heat balance at steady state, the total heat-transfer rate from a differential length dz of the fuel element, Fig. 2, must be equal to the total heat-generation rate of the length dz of the fuel element, so that

$$dQ_T dz = 2\pi r q_v dr dz \qquad (b)$$

Combining this and Eq. 5.2 and integrating between $r = r_i$ and $r = r_o$ of the fuel zone, we have

$$Q_T = 2\pi \int_{r_i}^{r_o} \frac{q_1}{\Sigma_{a_1}} \left[g_1 I_0(\varkappa_0 r) - g_2 K_0(\varkappa_0 r) \right] r dr$$

$$= \frac{2\pi}{\varkappa_0} \frac{q_1}{\Sigma_{a_1}} \left[g_1 \{ r_o I_1(\varkappa_0 r_o) - r_i I_1(\varkappa_0 r_i) \} - g_2 \{ r_o K_1(\varkappa_0 r_o) - r_i K_0(\varkappa_0 r_i) \} \right] \qquad (5.4)$$

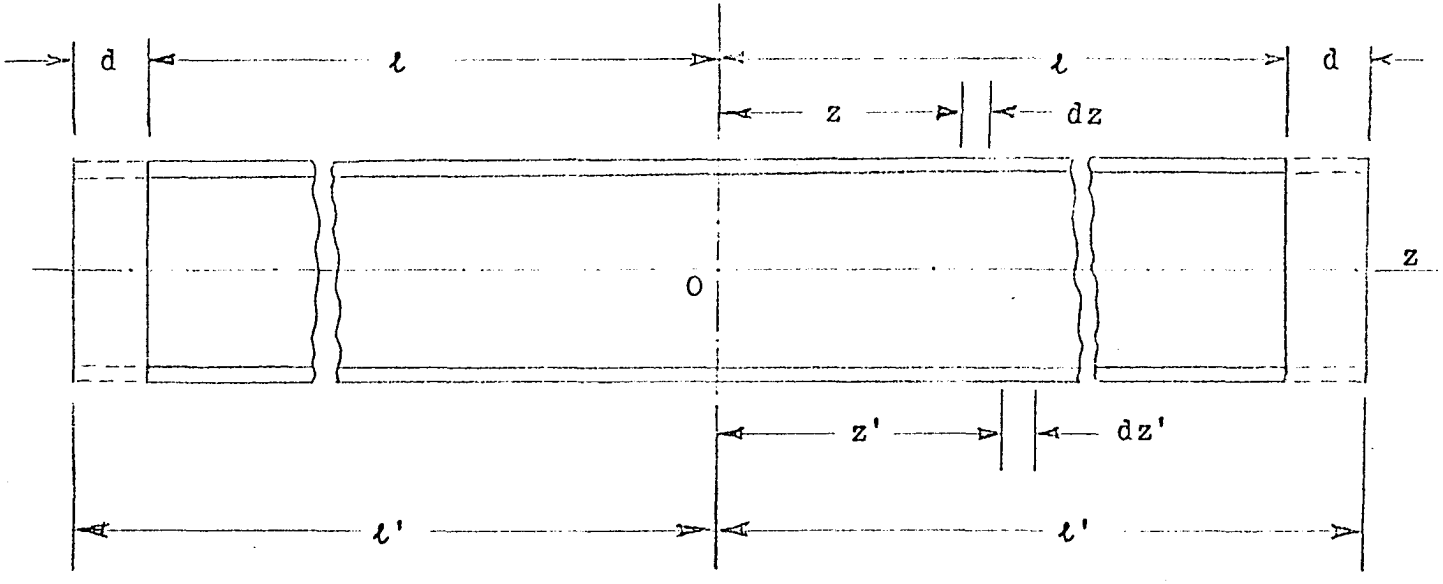

Fig. 2. The cylindrical fuel element

Now, for the case of symmetric power distribution, the average rate of total heat transferred per unit length of the fuel element is defined by the relations

$$Q_{av} = \frac{\int_{-\ell}^{\ell} Q_T f(z)dz}{2\ell' f(z')} = \frac{Q_T \int_0^{\ell} f(z)dz}{\ell' f(z')}$$

or

$$Q_T = Q_{av}\ell' f(z') / \int_0^{\ell} f(z)dz \qquad (5.5)$$

where $f(z')$ is independent of z. By equating Eqs. 5.4 and 5.5, the value of Q_{av} is obtained

$$Q_{av} = \frac{2\pi}{\kappa_0}\cdot\frac{q_1}{\Sigma_{a_1}}\cdot \frac{g_1\{r_0 I_1(\kappa_0 r_0 - r_i I_1(\kappa_0 r_i)\} - g_2\{r_0 K_1(\kappa_0 r_0) - r_i K_1(\kappa_0 r_i)\}}{\ell' f(z') / \int_0^{\ell} f(z)dz}$$

$$= \frac{2\pi \int_0^{\ell} f(z)dz}{\kappa_0 \ell' f(z')} \frac{q_1}{\Sigma_{a_1}} \Big[g_1\{r_0 I_1(\kappa_0 r_0) - r_i I_1(\kappa_0 r_i)\} - g_2\{r_0 K_1(\kappa_0 r_0) - r_i K_1(\kappa_0 r_i)\} \Big] \qquad (5.6)$$

In most cases, the neutron flux as well as the heat generation rate is approximately a sinusoidal distribution along the longitudinal direction of the fuel element. In order to satisfy the boundary conditions, we take

$$f(z') = \cos \frac{\pi z'}{2\ell'} \qquad (c)$$

$$f(z) = \cos \frac{\pi z}{2\ell} \tag{d}$$

$$\int_0^{\ell} f(z)dz = \int_0^{\ell} \cos \frac{\pi z}{2\ell}\, dz = \frac{2\ell}{\pi} \tag{e}$$

By substituting (c) and (e) into Eq. 5.5, it yields

$$Q_T = \frac{\pi \ell' Q_{av}}{2\ell} \cos \frac{\pi z'}{2\ell'} = Q_{max} \cos \frac{\pi z'}{2\ell'} \tag{5.7}$$

where, for this particular case, the maximum total heat generation rate per unit length of the fuel element at its center is

$$Q_{max} = \frac{\pi \ell'}{2\ell} Q_{av} \tag{5.8}$$

in which the value of Q_{av} is given by Eq. 5.6.

It is seen from the above discussion that for a given distribution of the neutron flux, the rate of heat generation per unit volume in the fuel can be obtained from Eq. 5.2. Subsequently, the average or maximum total heat-generation rate per unit length of the fuel element used in reactor design can be determined from Eq. 5.6 or 5.8.

In general, the variation of neutron flux distribution as well as of the heat generation rate along the longitudinal axis of the fuel element is small compared to that in the radial direction across the thickness of the fuel element.

VI. TEMPERATURE DISTRIBUTION IN THE FUEL ELEMENT WITH INTERNAL HEAT GENERATION

A. The Heat Conduction Equations

The basic equation for heat conduction with an internal heat source at steady state is given by

$$k \nabla^2 \theta + q_v = 0 \qquad (6.1)$$

where $\theta = T - T_0$ = effective or excess temperature

T_0 = ambient or reference temperature

T = variable temperature

k = thermal conductivity

q_v = internal volumetric heat source, or the heat generation rate per unit volume as defined previously

Eq. 6.1 is known as Poisson's equation of heat conduction. Expressions in the same form of the Poisson equation have been widely used in various fields of science and technology.

As usual, in the analysis of temperature distribution as well as the stress distribution in the fuel element, for simplicity, it is necessary to assume that

1. The thermal conductivity, k, is constant within a moderate range of temperature variation.
2. The length of the fuel element is much greater than its mean radius.

3. The heat generation is uniform throughout the thin fuel zone.

Based on these assumptions and by radial symmetry, Eq. 6.1 can be written as

$$\frac{d^2\theta}{dr^2} + \frac{1}{r}\frac{d\theta}{dr} = -\frac{q_v}{k} \tag{6.2}$$

or

$$\frac{1}{r}\frac{d}{dr}\left(r\frac{d\theta}{dr}\right) = -\frac{q_v}{k}$$

Integration of this from $r = r_i$ to any point r in the fuel zone yields

$$r\frac{d\theta}{dr} = r_i\left(\frac{d\theta}{dr}\right)_{r=r_i} - \frac{1}{k}\int_{r_i}^{r} q_v r\,dr \tag{6.3}$$

$$\theta = \theta_{r_i} + r_i\left(\frac{d\theta}{dr}\right)_{r=r_i} \ln\frac{r}{r_i} - \frac{1}{k}\int_{r_i}^{r}\frac{1}{r}\int_{r_i}^{r} q_v r\,dr\,dr \tag{6.4}$$

where θ_{r_i} = effective temperature at r_i of the fuel zone. To evaluate the quantity $r_i\left(\frac{d\theta}{dr}\right)_{r=r_i}$, the outer radius, r_0, of the fuel zone may be substituted for the upper limit r in Eq. 6.3, hence

$$r_i\left(\frac{d\theta}{dr}\right)_{r=r_i} = r_0\left(\frac{d\theta}{dr}\right)_{r=r_0} + \frac{1}{k}\int_{r_i}^{r_0} q_v r\,dr \tag{6.5}$$

Further, the fundamental relation for one-dimensional heat conduction, which is often called Fourier's equation, can be given by

$$Q = - kA \frac{d\theta}{dr} \tag{6.6}$$

where Q = rate of heat flow by conduction

A = cross sectional area perpendicular to the direction of heat flow

$d\theta/dr$ = effective temperature gradient in the radial direction

k = thermal conductivity, as defined previously

Upon substitution, the rates of heat flow per unit length on the inner and outer surface of the fuel element, Q_{r_i} and Q_{r_o}, become

$$Q_{r_i} = - 2\pi r_i k \left(\frac{d\theta}{dr}\right)_{r=r_i} = \beta Q_T \qquad \text{at } r = r_i \tag{6.6a}$$

$$Q_{r_o} = - 2\pi r_o k \left(\frac{d\theta}{dr}\right)_{r=r_o} = (1 - \beta) Q_T \qquad \text{at } r = r_o \tag{6.6b}$$

and

$$Q_T = Q_{r_i} + Q_{r_o} \tag{6.7}$$

in which Q_T = total rate of heat flow or heat generation per unit length of the fuel element as defined previously

β = fraction of the heat-flow rate goes into the inner passage of the fuel element, $0 < \beta < 1$.

If Q_T is eliminated from Eqs. 6.6a and 6.6b, this results

$$r_i \left(\frac{d\theta}{dr}\right)_{r=r_i} = -r_o \left(\frac{d\theta}{dr}\right)_{r=r_o} \frac{Q_{r_i}}{Q_{r_o}} = -r_o \left(\frac{d\theta}{dr}\right)_{r=r_o} \frac{\beta}{1 - \beta} \tag{6.8}$$

or

$$r_o \left(\frac{d\theta}{dr}\right)_{r=r_o} = -r_i \left(\frac{d\theta}{dr}\right)_{r=r_i} \frac{Q_{r_o}}{Q_{r_i}} = -r_i \left(\frac{d\theta}{dr}\right)_{r=r_i} \frac{1 - \beta}{\beta}$$

From Eq. 6.5 and the first of Eqs. 6.8, it yields

$$r_i \left(\frac{d\theta}{dr}\right)_{r=r_i} = \frac{\beta}{k} \int_{r_i}^{r_o} q_v r dr \tag{6.9}$$

in which β can be obtained from the heat transfer analysis. By introducing Eq. 6.9 into Eqs. 6.3 and 6.4, it follows that

$$r \frac{d\theta}{dr} = \frac{\beta}{k} \int_{r_i}^{r_o} q_v r dr - \frac{1}{k} \int_{r_i}^{r} q_v r dr \tag{6.3a}$$

$$\theta = \theta_{r_i} + \frac{\beta}{k} \ln \frac{r}{r_i} \int_{r_i}^{r_o} q_v r dr - \frac{1}{k} \int_{r_i}^{r} \frac{1}{r} \int_{r_i}^{r} q_v r dr dr \tag{6.4a}$$

when the effective temperature at the inner radius, θ_{r_i}, is given. In the same manner, by integrating Eqs. 6.2 and 6.3 from $r = r_o$ to any point r, the similar equations for thermal gradient and temperature distribution in the fuel zone can be obtained.

$$r \frac{d\theta}{dr} = r_o \left(\frac{d\theta}{dr}\right)_{r=r_o} + \frac{1}{k} \int_{r}^{r_o} q_v r dr \tag{6.10}$$

$$\theta = \theta_{r_o} + r_o \left(\frac{d\theta}{dr}\right)_{r=r_o} \ln \frac{r_o}{r} + \frac{1}{k} \int_{r}^{r_o} \frac{1}{r} \int_{r}^{r_o} q_v r dr dr \tag{6.11}$$

$$\theta = \theta_{r_o} + r_i \left(\frac{d\theta}{dr}\right)_{r=r_i} \ln \frac{r_o}{r} - \frac{1}{k} \int_{r}^{r_o} \frac{1}{r} \int_{r_i}^{r} q_v r dr dr \tag{6.12}$$

when the effective temperature at the outer radius, θ_{r_o}, is known. Substitution of Eqs. 6.8 into Eqs. 6.10, 6.11 and 6.12 respectively yields

$$r\frac{d\theta}{dr} = -\frac{1-\beta}{\beta} r_i \left(\frac{d\theta}{dr}\right)_{r=r_i} + \frac{1}{k}\int_r^{r_o} q_v r dr \qquad (6.10a)$$

$$\theta = \theta_{r_o} - \frac{1-\beta}{k} \ln\frac{r_o}{r}\int_{r_i}^{r_o} q_v r dr + \frac{1}{k}\int_r^{r_o}\frac{1}{r}\int_r^{r_o} q_v r dr dr \qquad (6.11a)$$

$$\theta = \theta_{r_o} - \frac{\beta}{k} \ln\frac{r_o}{r}\int_{r_i}^{r_o} q_v r dr + \frac{1}{k}\int_r^{r_o}\frac{1}{r}\int_{r_i}^{r} q_v r dr dr \qquad (6.12a)$$

Further, by integrating Eq. 6.3 between the limits $r = r_i$ and $r = r_o$ and using Eq. 6.9, a relation for the temperature difference between the inner and outer surface of the fuel zone can be obtained. Hence

$$\theta_{r_o} - \theta_{r_i} = \frac{\beta}{k} \ln\frac{r_o}{r_i}\int_{r_i}^{r_o} q_v r dr - \frac{1}{k}\int_{r_i}^{r_o}\frac{1}{r}\int_{r_i}^{r} q_v r dr dr \qquad (6.13)$$

Also, by differentiating Eq. 6.4a with respect to r, we have the thermal gradient for the fuel zone

$$\frac{d\theta}{dr} = \frac{\beta}{kr}\int_{r_i}^{r_o} q_v r dr - \frac{1}{k}\frac{d}{dr}\int_{r_i}^{r}\frac{1}{r}\int_{r_i}^{r} q_v r dr dr \qquad (6.14)$$

Since at the point where the maximum temperature in the fuel zone occurs the slope of thermal gradient vanishes, so that

the radius r for the maximum effective temperature, θ_{max}, within the fuel zone is

$$(r)_{\theta_{max}} = \beta\int_{r_i}^{r_o} q_v r dr \Big/ \frac{d}{dr}\int_{r_i}^{r}\frac{1}{r}\int_{r_i}^{r} q_v r dr dr \qquad (6.15)$$

Substituting this value of r into Eq. 6.4a the maximum effective temperature as well as the maximum temperature of the fuel element can be determined.

As pointed out in Section IV that there are two particular cases:

1. The fuel element is externally cooled only, for which

$$\beta = 0$$

2. The fuel element is internally cooled only, for which

$$\beta = 1$$

In case 1, Eqs. 6.4a, 6.12a and 6.13 reduce to

$$\theta = \theta_{r_i} - \frac{1}{k}\int_{r_i}^{r}\frac{1}{r}\int_{r_i}^{r} q_v r dr dr \qquad (6.4b)$$

$$\theta = \theta_{r_o} + \frac{1}{k}\int_{r}^{r_o}\frac{1}{r}\int_{r_i}^{r} q_v r dr dr \qquad (6.12b)$$

$$\theta_{r_o} - \theta_{r_i} = -\frac{1}{k}\int_{r_i}^{r_o}\frac{1}{r}\int_{r_i}^{r} q_v r dr dr \qquad (6.13a)$$

In case 2, Eqs. 6.4a, 6.12a and 6.13 become

$$\theta = \theta_{r_i} + \frac{1}{k} \ln \frac{r}{r_i} \int_{r_i}^{r_o} q_v r dr - \frac{1}{k} \int_{r_i}^{r} \frac{1}{r} \int_{r_i}^{r} q_v r dr dr \qquad (6.4c)$$

$$\theta = \theta_{r_o} - \frac{1}{k} \ln \frac{r_o}{r} \int_{r_i}^{r_o} q_v r dr + \frac{1}{k} \int_{r}^{r_o} \frac{1}{r} \int_{r_i}^{r} q_v r dr dr \qquad (6.12c)$$

$$\theta_{r_o} - \theta_{r_i} = \frac{1}{k} \ln \frac{r_o}{r_i} \int_{r_i}^{r_o} q_v r dr - \frac{1}{k} \int_{r_i}^{r_o} \frac{1}{r} \int_{r_i}^{r} q_v r dr dr \qquad (6.13b)$$

In summary, if the effective temperature θ_{r_i} or θ_{r_o} is known, or the temperature difference, $\theta_{r_o} - \theta_{r_i}$, is interested, with given values for k, β and prescribed functions of r for q_v, the temperature distribution in the fuel material of both internally and externally cooled fuel elements can, therefore, be determined from Eqs. 6.4a, 6.12a and 6.13, for which

$$0 < \beta < 1$$

In the particular case, the fuel element is externally cooled only, for which $\beta = 0$, the temperature distribution in the fuel material can be simply determined from Eqs. 6.4b, and 6.12b.

Finally, in another particular case, the fuel element is internally cooled only, for which $\beta = 1$, the temperature distribution in the fuel material can therefore be determined from Eqs. 6.4c and 6.12c. The effective temperature differ-

ence, $\theta_{r_0} - \theta_{r_i}$, can be found from Eq. 6.13b.

B. Exact Solution: The Modified Bessel-Function Distribution of Neutron Flux Across Thickness of the Fuel Zone

An exact solution for the temperature distribution in the fuel zone may be developed by using the modified Bessel functions for the neutron flux distribution. In doing so, Eq. 5.2 is introduced into Eqs. 6.4a, 6.12a and 6.13 for both internally and externally cooled fuel elements and the resulting expressions integrated, thus

$$\theta = \theta_{r_i} + \frac{q_1}{\Sigma_{a_1}} \frac{\beta}{k} \ln \frac{r}{r_i} \frac{1}{\varkappa_0} \Big[g_1 \{ r_0 I_1(\varkappa_0 r_0) - r_i I_1(\varkappa_0 r_i) \} - g_2 \{ r_0 K_1(\varkappa_0 r_0) - r_i K_1(\varkappa_0 r_i) \} \Big]$$
$$- \frac{q_1}{\Sigma_{a_1}} \frac{1}{k} \frac{1}{\varkappa_0} \Big[g_1 \{ \frac{1}{\varkappa_0} I_2(\varkappa_0 r) - \frac{1}{\varkappa_0} I_2(\varkappa_0 r_i) - r_i I_1(\varkappa_0 r_i) \ln \frac{r}{r_i} \}$$
$$+ g_2 \{ \frac{1}{\varkappa_0} K_2(\varkappa_0 r) - \frac{1}{\varkappa_0} K_2(\varkappa_0 r_i) + r_i K_1(\varkappa_0 r_i) \ln \frac{r}{r_i} \} \Big] \tag{6.16}$$

$$\theta = \theta_{r_0} - \frac{q_1}{\Sigma_{a_1}} \frac{\beta}{k} \ln \frac{r_0}{r} \frac{1}{\varkappa_0} \Big[g_1 \{ r_0 I_1(\varkappa_0 r_0) - r_i I_1(\varkappa_0 r_i) \} - g_2 \{ r_0 K_1(\varkappa_0 r_0) - r_i K_1(\varkappa_0 r_i) \} \Big] \tag{6.17}$$

$$- \frac{q_1}{\Sigma_{a_1}} \frac{1}{k} \frac{1}{\varkappa_0} \Big[g_1 \{ \frac{1}{\varkappa_0} I_2(\varkappa_0 r_0) - \frac{1}{\varkappa_0} I_2(\varkappa_0 r) - r_i I_1(\varkappa_0 r_i) \ln \frac{r_0}{r} \}$$

$$+ g_2 \{ \frac{1}{\varkappa_0} K_2(\varkappa_0 r_0) - \frac{1}{\varkappa_0} K_2(\varkappa_0 r) + r_i K_1(\varkappa_0 r_i) \ln \frac{r_0}{r} \} \Big]$$

$$\theta_{r_0} - \theta_{r_i} = \frac{q_1}{\Sigma_{a_1}} \frac{\beta}{k} \ln \frac{r_0}{r_i} \frac{1}{\varkappa_0} \Big[g_1 \{ r_0 I_1(\varkappa_0 r_0) - r_i I_1(\varkappa_0 r_i) \}$$

$$- g_2 \{ r_0 K_1(\varkappa_0 r_0) - r_i K_1(\varkappa_0 r_i) \} \Big]$$

$$- \frac{q_1}{\Sigma_{a_1}} \frac{1}{k} \frac{1}{\varkappa_0} \Big[g_1 \{ \frac{1}{\varkappa_0} I_2(\varkappa_0 r_0) - \frac{1}{\varkappa_0} I_2(\varkappa_0 r_i) \qquad (6.18)$$

$$- r_i I_1(\varkappa_0 r_i) \ln \frac{r_0}{r_i} \}$$

$$+ g_2 \{ \frac{1}{\varkappa_0} K_2(\varkappa_0 r_0) - \frac{1}{\varkappa_0} K_2(\varkappa_0 r_i) + r_i K_1(\varkappa_0 r_i) \ln \frac{r_0}{r_i} \} \Big]$$

for the values

$$0 < \beta < 1$$

and for θ_{r_i} or θ_{r_0} is known, or the temperature difference, $\theta_{r_0} - \theta_{r_i}$, is interested.

In the two particular cases:

1. the fuel element is externally cooled, $\beta = 0$
2. the fuel element is internally cooled, $\beta = 1$.

Then Eqs. 6.16, 6.17 and 6.18 are respectively reduced to

$$\theta = \theta_{r_i} - \frac{q_1}{\Sigma_{a_1}} \frac{1}{k} \frac{1}{\varkappa_0}\Big[g_1\{\frac{1}{\varkappa_0} I_2(\varkappa_0 r) - \frac{1}{\varkappa_0} I_2(\varkappa_0 r_i) - r_i I_1(\varkappa_0 r_i)\ln \frac{r}{r_i}\} + g_2\{\frac{1}{\varkappa_0} K_2(\varkappa_0 r) - \frac{1}{\varkappa_0} K_2(\varkappa_0 r_i) + r_i K_1(\varkappa_0 r_i)\ln \frac{r}{r_i}\} \Big] \qquad (6.16a)$$

$$\theta = \theta_{r_o} - \frac{q_1}{\Sigma_{a_1}} \frac{1}{k} \frac{1}{\varkappa_0}\Big[g_1\{\frac{1}{\varkappa_0} I_2(\varkappa_0 r_o) - \frac{1}{\varkappa_0} I_2(\varkappa_0 r) - r_i I_1(\varkappa_0 r_i)\ln \frac{r_o}{r}\} + g_2\{\frac{1}{\varkappa_0} K_2(\varkappa_0 r_o) - \frac{1}{\varkappa_0} K_2(\varkappa_0 r) + r_i K_1(\varkappa_0 r_i)\ln \frac{r_o}{r}\} \Big] \qquad (6.17a)$$

$$\theta_{r_o} - \theta_{r_i} = - \frac{q_1}{\Sigma_{a_1}} \frac{1}{k} \frac{1}{\varkappa_0}\Big[g_1\{\frac{1}{\varkappa_0} I_2(\varkappa_0 r_o) - \frac{1}{\varkappa_0} I_2(\varkappa_0 r_i) - r_i I_1(\varkappa_0 r_i)\ln \frac{r_o}{r_i}\} + g_2\{\frac{1}{\varkappa_0} K_2(\varkappa_0 r_o) - \frac{1}{\varkappa_0} K_2(\varkappa_0 r_i) + r_i K_1(\varkappa_0 r_i)\ln \frac{r_o}{r_i}\} \Big] \qquad (6.18a)$$

for the externally cooled fuel element; and

$$\theta = \theta_{r_i} + \frac{q_1}{\Sigma_{a_1}} \frac{1}{k} \ln \frac{r}{r_i} \frac{1}{\varkappa_0}\Big[g_1\{r_o I_1(\varkappa_0 r_o) - r_i I_1(\varkappa_0 r_i)\} - g_2\{r_o K_1(\varkappa_0 r_o) - r_i K_1(\varkappa_0 r_i)\} \Big] \qquad (6.16b)$$

$$- \frac{q_1}{\Sigma_{a_1}} \frac{1}{k} \frac{1}{\varkappa_0}\Big[g_1\{\frac{1}{\varkappa_0} I_2(\varkappa_0 r) - \frac{1}{\varkappa_0} I_2(\varkappa_0 r_i) - r_i I_1(\varkappa_0 r_i)\ln \frac{r}{r_i}\}$$

$$+ g_2\{\frac{1}{\varkappa_0} K_2(\varkappa_0 r) - \frac{1}{\varkappa_0} K_2(\varkappa_0 r_i) + r_i K_1(\varkappa_0 r_i) \ln \frac{r}{r_i}\} \Big]$$

$$\theta = \theta_{r_0} - \frac{q_1}{\Sigma_{a_1}} \frac{1}{k} \frac{1}{\varkappa_0} \ln \frac{r_0}{r} \frac{1}{\varkappa_0} \Big[g_1\{r_0 I_1(\varkappa_0 r_0) - r_i I_1(\varkappa_0 r_i)\}$$

$$- g_2\{r_0 K_1(\varkappa_0 r_0) - r_i K_1(\varkappa_0 r_i)\} \Big] \qquad (6.17b)$$

$$- \frac{q_1}{\Sigma_{a_1}} \frac{1}{k} \frac{1}{\varkappa_0} \Big[g_1\{\frac{1}{\varkappa_0} I_2(\varkappa_0 r_0) - \frac{1}{\varkappa_0} I_2(\varkappa_0 r) - r_i I_1(\varkappa_0 r_i) \ln \frac{r_0}{r}\}$$

$$+ g_2\{\frac{1}{\varkappa_0} K_2(\varkappa_0 r_0) - \frac{1}{\varkappa_0} K_2(\varkappa_0 r) + r_i K_1(\varkappa_0 r_i) \ln \frac{r_0}{r}\} \Big]$$

$$\theta_{r_0} - \theta_{r_i} = \frac{q_1}{\Sigma_{a_1}} \frac{1}{k} \ln \frac{r_0}{r_i} \frac{1}{\varkappa_0} \Big[g_1\{r_0 I_1(\varkappa_0 r_0) - r_i I_1(\varkappa_0 r_i)\}$$

$$- g_2\{r_0 K_1(\varkappa_0 r_0) - r_i K_1(\varkappa_0 r_i)\} \Big]$$

$$- \frac{q_1}{\Sigma_{a_1}} \frac{1}{k} \frac{1}{\varkappa_0} \Big[g_1\{\frac{1}{\varkappa_0} I_2(\varkappa_0 r_0) - \frac{1}{\varkappa_0} I_2(\varkappa_0 r_i) \qquad (6.18b)$$

$$- r_i I_1(\varkappa_0 r_i) \ln \frac{r_0}{r_i}\} + g_2\{\frac{1}{\varkappa_0} K_2(\varkappa_0 r_0) - \frac{1}{\varkappa_0} K_2(\varkappa_0 r_i)$$

$$+ r_i K_1(\varkappa_0 r_i) \ln \frac{r_0}{r_i}\} \Big]$$

for the internally cooled fuel element; where

$I_1(\varkappa_0 r_i)$ ≡ the modified Bessel function of the first kind of the first order, as defined before

$K_1(\varkappa_0 r_i)$ ≡ the modified Bessel function of the second kind of the first order, as defined previously

$I_2(\varkappa_0 r_0)$, $I_2(\varkappa_0 r_i)$, $I_2(\varkappa_0 r)$ ≡ the modified Bessel functions of the first kind of the second order

$K_2(\varkappa_0 r_0)$, $K_2(\varkappa_0 r_i)$, $K_2(\varkappa_0 r)$ ≡ the modified Bessel functions of the second kind of the second order

C. Approximate Solution: The Exponential or Parabolic Function Distribution of Neutron Flux Across Thickness of the Fuel Zone

The preceding analysis for the temperature distribution in the fuel material resulting from the modified Bessel function distribution of the neutron flux across the thickness of the fuel zone is tedious and unwieldy when the temperature distribution is to be used in the creep analysis for stress distribution in the fuel element. At the same time, experiments show that the observed neutron flux distributions do not agree exactly with the theoretical solution obtained from the simple diffusion theory. Therefore, it is desirable to examine the nature of the modified Bessel functions closely and to find a reasonably simplified solution for the neutron flux distribution which will approximately satisfy available experimental results and yield sufficiently accurate temperature distribution for the creep analysis of the fuel element. This will further be useful to deal with the mechanical stability

of the fuel element.

The nature of these modified Bessel or cylindrical functions such as $I_0(\varkappa_0 r)$, $K_0(\varkappa_0 r)$ etc. are not of the oscillating type as those Bessel functions obtained from the Bessel equation. The behavior of these modified Bessel functions is essentially the exponential functions when their asymptotic approximations are concerned (17). For instance, when the argument or radius r becomes large, the modified Bessel functions of the first and second kinds of the zero order, $I_0(r)$ and $K_0(r)$, can, respectively, be expressed as

$$I_0(r) \cong (2\pi r)^{-1/2} e^r = (2\pi r)^{-1/2}\left(1 + r + \frac{r^2}{2!} + \cdots\right) \qquad (6.19)$$

$$K_0(r) \cong (\pi/2r)^{1/2} e^{-r} = (\pi/2r)^{1/2}\left(1 - r + \frac{r^2}{2!} - \cdots\right) \qquad (6.20)$$

Some similar expressions in the same nature can be obtained for the modified Bessel functions of the higher orders.

Based on the foregoing discussion and the practical consideration, it will be sufficiently accurate to represent the neutron flux distribution over the thickness of the fuel zone by combining the solutions of the modified Bessel functions, Eqs. 5.2, 6.19 and 6.20 into the relatively simple form

$$\phi_0 = a_0\left[1 + b(r - c_0)^2\right] \quad r_i \leq r \leq r_0 \qquad (6.21)$$

where a_0, b and c_0 are constants. These constants can be

readily determined with any three points selected from an experimental neutron flux ϕ versus radius r curve if the geometric and material arrangements in the experiment are identical to the fuel element under consideration. This approach is similar to the kernel method used to establish some basic equations of the transport or high-order diffusion theory (instead of solving the Boltzmann transport equations analytically) for which the slowing-down kernel of neutron flux distribution can be measured experimentally (18).

Now, introducing Eq. 5.1 into Eq. 6.21, the rate of heat generation per unit volume, q_v, induced by the neutron flux becomes

$$q_v = a_0 \Sigma_f E_f \left[1 + b(r - c_0)^2 \right] = a \left[1 + b r_0^2 (x - c)^2 \right] \quad (6.22)$$

in which

$$a = a_0 \Sigma_f E_f = \text{constant}$$
$$x = r/r_0, \quad c = c_0/r_0 \quad (6.23)$$

As before, for the externally and internally cooled fuel element, by substituting Eq. 6.22 into Eqs. 6.4a, 6.12a and 6.13 and integrating between the respective limits, the radial temperature distribution and the temperature difference between the inner and outer surface of the fuel zone are respectively obtained.

$$\theta = \theta_{r_i} + \frac{a\beta}{2k} M_1 \ln \frac{x}{x_i} - \frac{a}{2k}\Big[(1 + br_0^2c^2)(\frac{x^2}{2} - x_i^2 \ln \frac{x}{x_i}) + br_0^2\{x^3(\frac{x}{8} - \frac{4c}{9}) - x_i^3(\frac{x_i}{2} - \frac{4c}{3})\ln \frac{x}{x_i}\} - M_2 \Big] \tag{6.24}$$

$$\theta = \theta_{r_0} - \frac{a\beta}{2k} M_1 \ln \frac{1}{x} + \frac{a}{2k}\Big[M_3 - (1 + br_0^2c^2)(\frac{x^2}{2} - x_i^2 \ln \frac{1}{x}) - br_0^2\{x^3(\frac{x}{8} - \frac{4c}{9}) - x_i^3(\frac{x_i}{2} - \frac{4c}{3})\ln \frac{1}{x}\} \Big] \tag{6.25}$$

$$\theta_{r_0} - \theta_{r_i} = \frac{a\beta}{2k} M_1 \ln \frac{1}{x_i} - \frac{a}{2k} M_4 \tag{6.26}$$

where

$$x_i = r_i/r_0, \quad x = r/r_0$$

$$M_1 = \frac{1}{r_0^2}\Big[r_0^2 - r_i^2 + b\{\frac{1}{2}(r_0^4 - r_i^4) - \frac{4c_0}{3}(r_0^3 - r_i^3) + c_0^2(r_0^2 - r_i^2)\}\Big]$$

$$= (1 - x_i^2) + br_0^2\{\frac{1}{2}(1 - x_i^4) - \frac{4c}{3}(1 - x_i^3) + c^2(1 - x_i^2)\}$$

$$M_2 = \frac{1}{r_0^2}\{\frac{r_i^2}{2} + b(\frac{r_i^4}{8} - \frac{4r_i^3c_0}{9} + c_0^2\frac{r_i^2}{2})\}$$

$$= \frac{x_i^2}{2}\{1 + br_0^2(\frac{x_i^2}{4} - \frac{8x_ic}{9} + c^2)\} \tag{6.27}$$

$$M_3 = \frac{1}{2}\left[1 + b\left(\frac{r_0^2}{4} - \frac{8r_0c_0}{9} + c_0^2\right) \right] = \frac{1}{2}\left[1 + br_0^2\left(\frac{1}{4} - \frac{8c}{9} + c^2\right) \right]$$

$$M_4 = \frac{1}{2r_0^2}\left[\frac{r_0^2 - r_i^2}{2} - r_i^2 \ln \frac{r_0}{r_i} + b\left\{\frac{1}{2}\left(\frac{r_0^4 - r_i^4}{4} - r_i^4 \ln \frac{r_0}{r_i}\right)\right.\right.$$

$$\left.\left. - \frac{4c_0}{3}\left(\frac{r_0^3 - r_i^3}{3} - r_i^3 \ln \frac{r_0}{r_i}\right) + c_0^2\left(\frac{r_0^2 - r_i^2}{2} - r_i^2 \ln \frac{r_0}{r_i}\right)\right\} \right]$$

$$= \frac{1}{2}\left[\frac{1 - x_i^2}{2} - x_i^2 \ln \frac{1}{x_i} + br_0^2\left\{\frac{1}{2}\left(\frac{1 - x_i^4}{4} - x_i^4 \ln \frac{1}{x_i}\right)\right.\right.$$

$$\left.\left. - \frac{4c}{3}\left(\frac{1 - x_i^3}{3} - x_i^3 \ln \frac{1}{x_i}\right) + c^2\left(\frac{1 - x_i^2}{2} - x_i^2 \ln \frac{1}{x_i}\right)\right\} \right]$$

As discussed before, in the two particular cases:

1. If the fuel element is externally cooled only, $\beta = 0$,
2. If the fuel element is internally cooled only, $\beta = 1$,

so that Eqs. 6.24, 6.25 and 6.26 can be simplified accordingly.

VII. CREEP ANALYSIS FOR STRESS DISTRIBUTION IN THE FUEL ELEMENT

A. Introduction to the Creep Analysis

In the design and operation condition of high-power heterogeneous reactors using solid metallic, ceramic or dispersion fuel elements, the fuel elements are required to maintain their physical and mechanical integrity in order to keep the coolant from being contaminated with radioactive fission products. If severe ruptures take place in the fuel elements, flow channels of coolant around the fuel elements may be seriously blocked and structural damage caused by over-heating may occur within the reactor. For example, the failure and collapse of the cylindrical fuel elements in the Borax-IV boiling water reactor is a typical case of the mechanical instability of the fuel elements (19). Therefore, the classic thermoelastic analysis for the fuel element becomes inadequate.

In the creep analysis for stress distribution in the fuel element, a mathematical model which represents the physical and mechanical behavior of the fuel-element materials in operation conditions becomes necessary. This mathematical model is also termed the mechanical model or the material model of the fuel materials (20). When a fuel material is subjected to burn-up, irradiation, elevated temperature and

high stresses, a realistic mechanical model for the material must take the thermal and irradiation creep into consideration. In fact, creep rate and strain are greatly accelerated under the irradiation condition (13, 14), as particularly discussed before.

B. Basic Assumptions

In the creep analysis for stress distribution in the fuel element of power reactors at steady-state condition, the following basic assumptions are made:

1. Both fuel and cladding materials of the fuel element are in a perfectly plastic state, and their densities are approximately constant.
2. Both fuel and cladding materials under irradiation are approximately isotropic. That is, the fuel material only has moderate thermal cycling growth, irradiation growth and swelling.
3. The fuel and cladding materials follow Mises' yield criterion.
4. The metallic bonding between the fuel and cladding materials is perfectly integral.
5. The membrane theory is applicable to the cladding of the fuel element.
6. The cladding material under irradiation exhibits the

property of irradiation or strain hardening.

In order to simplify the creep analysis, under certain conditions, it may be further assumed that the stress and strain relations for the fuel element satisfy the state of plane strain.

The basic assumption 1 implies that the change in volume of the fuel material is approximately zero during creep and plastic flow, so that the equation of incompressibility is applicable.

From the basic assumption 2, it may be realized that the principal axes of creep strain rates must coincide with those of principal stress if the fuel material is approximately isotropic.

The Mises yield criterion (21) may be so defined that when the second stress invariant, J_2 (which will be considered later) or elastic distortion energy reaches a critical value the material begins to yield. For most metals the Mises criterion fits the experimental data very closely.

The basic assumption 4 means that the fuel and cladding materials are perfectly bonded and have equal stress and strain at the bonding surface.

The membrane theory in the basic assumption 5 refers usually to a thin shell, similar to a membrane, which can take uniform tension but is unable to resist any compression or bending moment. For very thin cladding of the cylindrical

fuel element, the action of the cladding is very close to a thin shell or analogous to a membrane.

Finally, the basic assumption 6 is self-evident. The degree of strain hardening of a cladding material depends mainly on total creep or plastic flow, intensity and time of irradiation. This basic assumption is justified from observation of the experiments.

C. General Equations for Creep Rate and Creep Strain

Creep of a solid material may be defined in a usual sense as a slow, continuous, plastic deformation of the material under a constant load and constant temperature, as given in Section IIIA. The effects of the thermal and irradiation creep on the stability of the fuel elements have been also discussed. In general, the creep behavior of a non-irradiated material differs greatly from that of an irradiated one because under irradiation the physical and mechanical properties of the material will change appreciably.

For a non-irradiated solid the creep rate has been assumed to be equal to the product of a function of effective stress, a function of temperature and a function of time (22). This assumption is justified by the observed data (23) and the derived mechanical model for non-irradiated beta-quenched uranium at elevated temperatures (24).

In spite of the irradiation effect and burn-up, on the basis of available experimental data (12, 25, 26), the effective creep rate, $\dot{\epsilon}$, of fuel elements can, to a great extent, be postulated as a function of effective stress, σ, irradiation temperature, T, and time of irradiation, t.

$$\dot{\epsilon} = \Psi\,(\sigma, t, T) \tag{7.1}$$

In other words, the effective creep rate can be conveniently written as the product of a function of effective stress, $F(\sigma)$, a function of irradiation temperature $g(T)$ and a function of irradiation time, $f(t)$

$$\dot{\epsilon} = F(\sigma)f(t)g(T) \tag{7.1a}$$

here the dot refers to a time rate on the basis of flow concept.

As to the function of irradiation temperature, by taking the radial temperature variation into account we further postulate that the temperature varies with radius r or x $(= r/r_0)$ of the fuel element under consideration (for example, see Eqs. 6.4a and 6.12). Hence

$$g(T) \equiv g\left[g_1(x)\right] \equiv f_1(x)$$

and, consequently, Eq. 7.1a becomes

$$\dot{\epsilon} = F(\sigma)f(t)f_1(x) \tag{7.1b}$$

At steady-state condition, the effective stress or $F(\sigma)$ does not vary with the irradiation time, t. This agrees with the definition of creep given above.

Another way, based on the deformation concept, to express the creep relations is that the effective creep strain, ϵ, is a function of the effective stress, irradiation temperature and the time of irradiation

$$\epsilon = \psi(\sigma, t, T) \tag{7.2}$$

Differentiating this with respect to the time t, it follows

$$\dot{\epsilon} = \partial \psi(\sigma, t, T)/\partial t \tag{7.3}$$

Now, eliminating t from Eqs. 7.2 and 7.3, we have the effective creep rate as a function of the effective stress, irradiation temperature and creep strain

$$\dot{\epsilon} = \psi_1(\sigma, \epsilon, T) \equiv F_1(\sigma)H(\epsilon)g(T) \tag{7.4}$$

Again, letting the radial temperature variation of the solid or the fuel element as a function x (= r/r_0), $g_2(x)$, and $g[g_2(x)] = f_2(x)$, it yields

$$\dot{\epsilon} = F_1(\sigma)H(\epsilon)f_2(x) \tag{7.4a}$$

where $F_1(\sigma)$, $H(\epsilon)$ and $f_2(x)$ are functions of effective stress, effective creep strain and radius of fuel element respectively. In order to agree with the definition of creep, ϵ must be

produced with a constant load during creep and plastic flow.

Furthermore, on the theoretical basis the relationships between the effective stress and the creep rate can be represented by the hyperbolic sine law which for high stresses can be simply reduced to the exponential law (27). In practice, however, almost all the creep test data have been represented by the power creep law. The reason for this practice is that when the σ versus $\dot{\epsilon}$ curve plotted in the log-log scale is simply a straight line.

Finally, it may be emphasized that, whether the material is irradiated or not, the basic relations represented by the general equations for creep rate and creep strain given above can be applied to any particular creep problem of interest.

D. Creep Analysis for the Cylindrical Fuel Element

For a cylindrical fuel element the relations between the radial, tangential creep strain rates, $\dot{\epsilon}_r$, $\dot{\epsilon}_t$, and the radial displacement rate, $\dot{u}_r$ or $\dot{u}$ $(= \dot{u}_r/r_0)$ of the fuel element at any radius r or x $(= r/r_0)$, based on the flow concept, are given by

$$\dot{\epsilon}_r = \partial\dot{u}/\partial x \tag{7.5}$$

$$\dot{\epsilon}_t = \dot{u}/x \tag{7.6}$$

where both $\dot{u}$ and x are non-dimensional. At the same time, the

known equation of compatibility in terms of the creep strain rates of the fuel element can be given by

$$x \frac{\partial \dot{\epsilon}_t}{\partial x} + \dot{\epsilon}_t - \dot{\epsilon}_r = \frac{\partial (x\dot{\epsilon}_t)}{\partial x} - \dot{\epsilon}_r = 0 \qquad (7.7)$$

Denoting the effective creep rate of the fuel element also in terms of the creep strain rates by the relation

$$\dot{\epsilon} = \frac{1}{2}(\dot{\epsilon}_r - \dot{\epsilon}_t) \qquad (7.8)$$

Eqs. 7.7 and 7.8 may be combined to give

$$x \frac{\partial \dot{\epsilon}_t}{\partial x} - 2\dot{\epsilon} = 0 \qquad (7.9)$$

Further, from the basic assumption 1, the equation of incompressibility for the components of the creep strain rate, $\dot{\epsilon}_r$, $\dot{\epsilon}_t$, $\dot{\epsilon}_z$ and the resultant rate of linear dilatations, $\dot{\epsilon}_R$, due partly to thermal expansion, $\alpha\theta$, and partly to thermal-cycling and radiation dilatation, ϵ_I, can be correlated together as

$$\dot{\epsilon}_r + \dot{\epsilon}_t + \dot{\epsilon}_z - 3\dot{\epsilon}_R = 0 \qquad (7.10)$$

and

$$\dot{\epsilon}_R = \alpha \dot{\theta} + \dot{\epsilon}_I \qquad (7.11)$$

where α = linear coefficient of thermal expansion

θ = effective or excess temperature as defined previously

$\dot{\theta}$ = rate of change in effective temperature

Introduction of Eqs. 7.5 and 7.6 into Eq. 7.10 gives

$$\dot{\epsilon}_r + \dot{\epsilon}_t = \frac{1}{x}\frac{\partial(x\dot{u})}{\partial x} = \frac{1}{x}\frac{\partial(x^2\dot{\epsilon}_t)}{\partial x} = 3\dot{\epsilon}_R - \dot{\epsilon}_z \qquad (7.12)$$

Similarly, on the basis of the deformation concepts, the corresponding expressions to Eqs. 7.5 through 7.12 can be respectively given by

$$\epsilon_r = \partial u/\partial x \qquad (7.5a)$$

$$\epsilon_t = u/x \qquad (7.6a)$$

$$\epsilon_r = \partial(x\epsilon_t)/\partial x = x\frac{\partial \epsilon_t}{\partial x} + \epsilon_t \qquad (7.7a)$$

$$\epsilon = \frac{1}{2}(\epsilon_r - \epsilon_t) \qquad (7.8a)$$

$$2\epsilon = x\,\partial\epsilon_t/\partial x \qquad (7.9a)$$

$$\epsilon_r + \epsilon_t + \epsilon_z - 3\epsilon_R = 0 \qquad (7.10a)$$

$$\epsilon_R = \alpha\,\theta + \epsilon_I \qquad (7.11a)$$

$$\epsilon_r + \epsilon_t = \frac{1}{x}\frac{\partial(xu)}{\partial x} = \frac{1}{x}\frac{\partial(x^2\epsilon_t)}{\partial x} = 3\epsilon_R - \epsilon_z \qquad (7.12a)$$

Either of the two sets of equations, similar to the general equations for creep rate and creep strain given above, can be used to solve the problem under consideration. In the further analysis, we shall use the set of equations based on the deformation concept.

Now, integrating Eq. 7.12a between x = 1 and an arbitrary

point x in the fuel zone, it follows

$$xu = (xu)_0 - \int_x^1 (3\epsilon_R - \epsilon_z)xdx \qquad x_i \leq x \leq 1$$

$$u = \frac{1}{x}\left[u_0 - \int_x^1 (3\epsilon_R - \epsilon_z)xdx \right] \tag{7.13}$$

or

$$\epsilon_t = \frac{u}{x} = \frac{\epsilon_{t0}}{x^2} - \frac{1}{x^2}\int_x^1 (3\epsilon_R - \epsilon_z)xdx \qquad x_i \leq x \leq 1 \tag{7.14}$$

where $u_0 = (xu)_0 = \epsilon_{t_0}$ = tangential strain at r_0 or $x = 1$

$x_i = r_i/r_0$ = ratio of inner radius to outer radius of the fuel zone

Introducing Eq. 7.14 into Eq. 7.7a and integrating from $x = 1$ to any point x in the fuel zone, it yields

$$\epsilon_r = -\frac{\epsilon_{t_0}}{x^2} + \frac{1}{x^2}\int_x^1 (3\epsilon_R - \epsilon_z)xdx - \frac{1}{x}\frac{\partial}{\partial x}\int_x^1 (3\epsilon_R - \epsilon_z)xdx$$

$$x_i \leq x \leq 1 \tag{7.15}$$

By substituting Eqs. 7.14 and 7.15 into Eq. 7.8a, the effective creep strain in the fuel zone becomes

$$\epsilon = -\frac{\epsilon_{t_0}}{x^2} + \frac{1}{x^2}\int_x^1 (3\epsilon_R - \epsilon_z)xdx - \frac{1}{2x}\frac{\partial}{\partial x}\int_x^1 (3\epsilon_R - \epsilon_z)xdx$$

$$x_i \leq x \leq 1 \tag{7.16}$$

in which u_0, ϵ_{t_0} and ϵ_z are constant. If ϵ_R is a given function of x, then u, ϵ_t, ϵ_r as well as ϵ can be evaluated from Eqs. 7.13 through 7.16 respectively.

On the basis of the plasticity theory, any yield criterion for a perfectly plastic material can be expressed in a general form (28),

$$f(J_1, J_2, J_3) = 0 \tag{7.17}$$

where J_1, J_2 and J_3 are the first three invariants of the stress tensor σ_{ij}, and the indices i and j usually take values of 1, 2 and 3 in the cartesian coordinates. For the cylindrical coordinate system the indices i and j refer to the radial, tangential and axial axes respectively. Therefore, for the problem under consideration, these invariants are defined in terms of the principal components of stress, σ_r, σ_t, σ_z by the relations

$$J_1 \equiv \sigma_r + \sigma_t + \sigma_z = 3\bar{\sigma} \tag{7.18}$$

$$\begin{aligned} J_2 &\equiv -(\sigma_r\sigma_t + \sigma_t\sigma_z + \sigma_z\sigma_r)^{1/2} \\ &= \left[\frac{3}{2}(s_r^2 + s_t^2 + s_z^2)\right]^{1/2} \\ &= \sqrt{3}(s^2 + \frac{3}{4}s_z^2)^{1/2} \end{aligned} \tag{7.19}$$

$$J_3 \equiv \sigma_r\sigma_t\sigma_z \tag{7.20}$$

where $\bar{\sigma} \equiv \frac{1}{3}(\sigma_r + \sigma_t + \sigma_z)$

$$s_r \equiv \sigma_r - \bar{\sigma}$$

$$s_t \equiv \sigma_t - \bar{\sigma} \qquad (7.21)$$

$$s_z \equiv \sigma_z - \bar{\sigma}$$

in which, by definition, $\bar{\sigma}$ is the mean normal stress, and s_r, s_t, s_z are respectively the components of stress deviation or deviatoric stress in the radial, tangential and axial directions.

Now, from the above discussion and the Mises yield criterion, the stress-strain relations for a perfectly plastic material under irradiation are given by

$$\epsilon_r - \epsilon_R = \lambda s_r = \lambda(s - \tfrac{1}{2} s_z)$$

$$\epsilon_t - \epsilon_R = \lambda s_t = -\lambda(s + \tfrac{1}{2} s_z) \qquad (7.22)$$

$$\epsilon_z - \epsilon_R = \lambda s_z$$

and

$$\epsilon = \lambda s$$

$$s = \tfrac{1}{2}(\sigma_r - \sigma_t), \quad \epsilon = \tfrac{1}{2}(\epsilon_r - \epsilon_t) \qquad (7.23)$$

where λ is a multiplier or a parameter, in general, $0 \leq \lambda \leq 1$, for $0 \leq x \leq 1$.

Substitution of the last of Eqs. 7.22 and the first of Eqs. 7.23 into Eq. 7.19 yields

$$\lambda = \frac{\sqrt{3}}{J_2}\left[\epsilon^2 + \frac{3}{4}(\epsilon_z - \epsilon_R)^2 \right]^{1/2} \qquad (7.24)$$

which is a function of the strain components. In turn, ϵ and ϵ_R are functions of r or x of the fuel zone. Also J_2 is generally a function of r or x. (Note, for simplicity, J_2 defined above differs from the conventional one.) For a given fuel material at a given irradiation temperature, however, J_2 may be considered a constant, i.e. the mean value of the second stress invariant. Since ϵ_{t_0} and ϵ_z are constant, Eq. 7.24 can be used to determine the parameter λ. Once the values of λ are evaluated, then from Eqs. 7.22 and 7.23, s_r, s_t, s_z and s can be found.

The known equation of equilibrium in the radial direction is given by

$$x \frac{d\sigma_r}{dx} + \sigma_r - \sigma_t = 0$$

or

$$x \frac{d\sigma_r}{dx} = -2s \qquad (7.25)$$

The equations of equilibrium in the tangential and axial directions make no contribution. By integrating this from $x = 1$ or from $x = x_i$ to any point x in the fuel zone, the radial stress produced in the fuel material is

$$\sigma_r = \sigma_{r_0} - 2 \int_1^x \frac{s\,dx}{x}$$

or

$$x_i \leq x \leq 1 \qquad (7.26)$$

$$\sigma_r = \sigma_{r_i} - 2\int_{x_i}^{x} \frac{s\,dx}{x}$$

where $s = \frac{1}{2}(\sigma_r - \sigma_t)$, given in Eq. 7.23

σ_{r_0}, σ_{r_i} = radial stresses at $x = 1$ and $x = x_i$ of the fuel zone respectively

Here, it should be noted that based on the basic assumption 4, for a perfectly metallic bonding, the radial stresses on the outer and inner surface of the fuel are, respectively, equal to that on the outer and inner cladding surface of the fuel element; or the boundary conditions for the radial stresses on the interface are

$$\begin{aligned} (\sigma_{r_0})_f &= (\sigma_{r_0})_c \quad \text{at} \quad x = 1 \\ (\sigma_{r_i})_f &= (\sigma_{r_i})_c \quad \text{at} \quad x = x_i \end{aligned} \tag{7.27}$$

in which the subscripts f and c refer respectively to the fuel and the cladding. This also holds true for the tangential and axial stresses.

To obtain the tangential stress, σ_t, in the fuel zone, Eqs. 7.25 and 7.26 or the second of Eqs. 7.23 may be employed. The latter yields

$$\sigma_t = \sigma_r - 2s \tag{7.28}$$

Furthermore, from Eqs. 7.21 the axial stress produced in the fuel zone becomes

$$\sigma_z = s_z + \bar{\sigma} = \frac{3}{2}\left[\sigma_z - \frac{1}{3}(\sigma_r + \sigma_t + \sigma_z)\right] - \frac{1}{2}(\sigma_r - \sigma_t) + \sigma_r$$

$$= \frac{3}{2} s_z - s + \sigma_r \qquad (7.29)$$

in which s_z, s and σ_r are, respectively, given by Eqs. 7.22 and 7.23 after the parameter λ has been evaluated from Eq. 7.24.

In summary, by using Eqs. 7.26, 7.28 and 7.29 the components of stress σ_r, σ_t and σ_z of the fuel zone can be obtained. The mechanical stability of a fuel element depends mainly upon the stress distribution in the fuel zone and the structural strength of the cladding.

In order to determine the stresses in the inner and outer cladding of the fuel element, the basic assumptions 4, 5 and 6, given previously, are to be employed.

On the basis of the basic assumption 4, when inner and outer cladding surfaces are perfectly integrated with inner and outer surfaces of the fuel zone, in addition to Eqs. 7.27, the boundary conditions of strain components ϵ_r, ϵ_t and ϵ_z also require, Fig 3a,

$$\begin{aligned} (\epsilon_{r_i})_f &= (\epsilon_{r_i})_c \\ (\epsilon_{t_i})_f &= (\epsilon_{t_i})_c \qquad \text{at} \quad x = x_i \\ (\epsilon_{z_i})_f &= (\epsilon_{z_i})_c \end{aligned} \qquad (7.30)$$

$$(\epsilon_{r_0})_f = (\epsilon_{r_0})_c$$

$$(\epsilon_{t_0})_f = (\epsilon_{t_0})_c \qquad \text{at} \quad x = 1 \qquad (7.31)$$

$$(\epsilon_{z_0})_f = (\epsilon_{z_0})_c$$

Further, from the basic assumption 5, the cladding of the fuel element is so thin (compared to the fuel) that the membrane theory is applicable. Consequently, the tangential stress, σ_{t_c}, across the thickness of the inner cladding is approximately uniform. The radial stress at the interface is σ_{r_i} and vanishes at the free surface. Therefore, the equilibrium of the radial forces acting on an element of the inner cladding as shown in Fig. 3b, becomes

$$\sigma_{r_i} r_0 x_i \cdot 1 \cdot \psi = (\sigma_{t_i})_c h_i \cdot 1 \cdot 2 \sin \frac{\psi}{2} \cong (\sigma_{t_i})_c h_i \psi$$

$$\sigma_{r_i} = h_i (\sigma_{t_i})_c / r_0 x_i \quad \text{at } x = x_i \qquad (7.32)$$

Similarly, the equilibrium of the radial forces acting on an element of the outer cladding, Fig. 3c, is

$$(\sigma_{t_0})_c = - \sigma_{r_0} r_0 / h_0 \quad \text{at} \quad x = 1 \qquad (7.33)$$

where σ_{r_0} = radial stress at the interface of the outer cladding and outer surface of the fuel zone

h_i = thickness of the inner cladding

h_0 = thickness of the outer cladding

The radial stress σ_{r_i} or σ_{r_0} can be readily determined

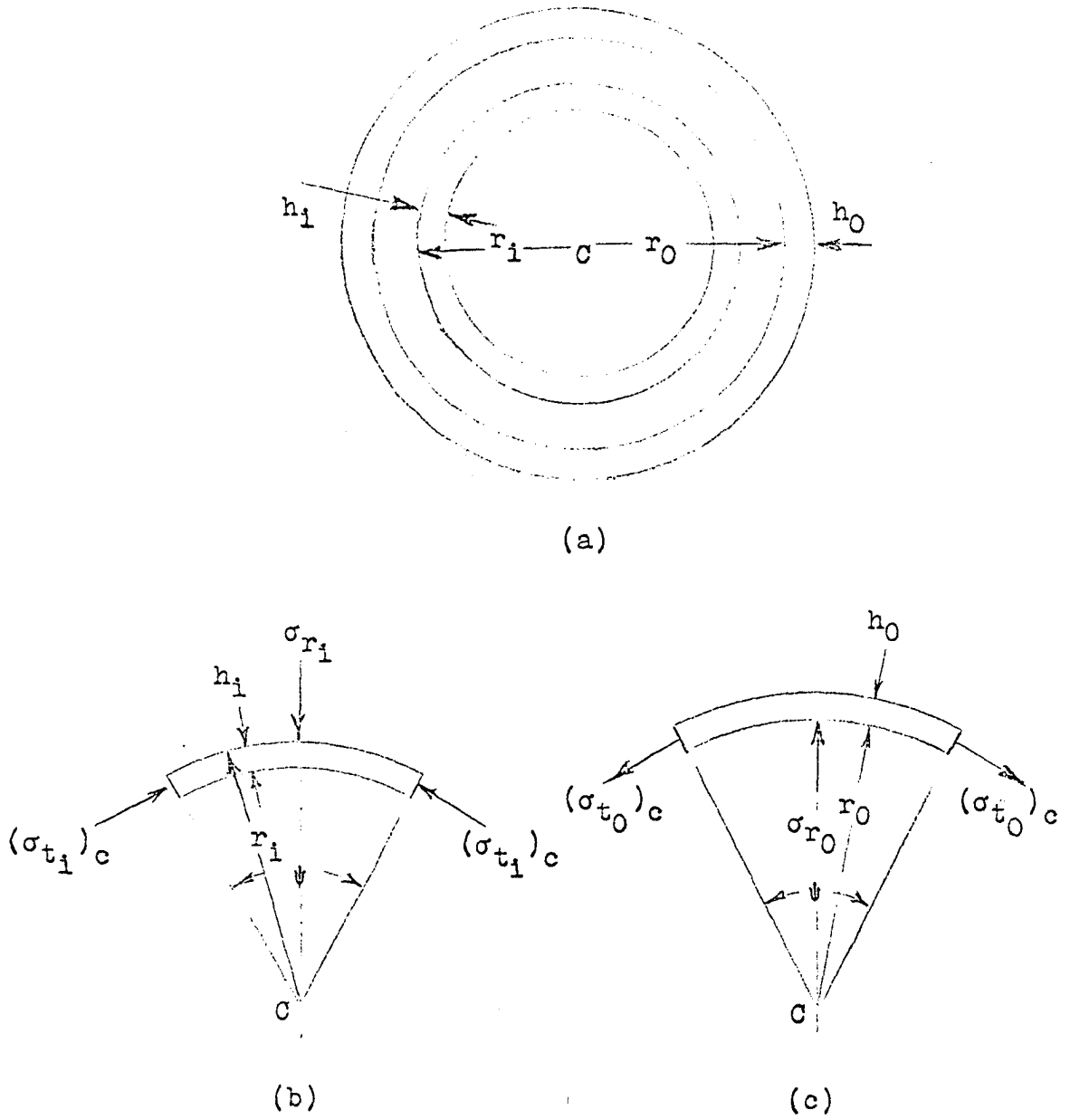

Fig. 3. Cross section of the cylindrical fuel element

when the corresponding tangential stress $(\sigma_{t_c})_i$ or $(\sigma_{t_c})_o$ has been found. Later, in the calculation for the stress distribution in the fuel zone, $(\sigma_{t_i})_c$ which is equal to $(\sigma_{t_i})_f$ at $x = x_i$, Eq. 7.27, will be determined from the Mises criterion of yielding for a cladding material of the fuel element. Then, σ_{r_i} in the second of Eqs. 7.26 will then be obtained from Eq. 7.32.

In most practical cases, cladding materials under irradiation and thermal cycling usually become radiation or irradiation hardening, but they will not produce any noticeable irradiation growth and swelling as the fuel material does. Therefore, for the cladding material Eq. 7.11a reduces to

$$\epsilon_R = \alpha_c \theta_c \tag{7.11b}$$

In order to take the radiation hardening of the cladding material into account, we again use the basic assumptions 1, 2 and 3 to formulate the stress-strain relations of the cladding. Hence, for the zero initial conditions, it follows that

$$\begin{aligned}
\epsilon_r - \alpha_c\theta_c = \mu s_r &= \mu\left(\frac{2\sigma_{r_c} - \sigma_{t_c} - \sigma_{z_c}}{3}\right) \\
\epsilon_t - \alpha_c\theta_c = \mu s_t &= \mu\left(\frac{2\sigma_{t_c} - \sigma_{z_c} - \sigma_{r_c}}{3}\right) \\
\epsilon_z - \alpha_c\theta_c = \mu s_z &= \mu\left(\frac{2\sigma_{z_c} - \sigma_{r_c} - \sigma_{t_c}}{3}\right)
\end{aligned} \tag{7.34}$$

and

$$J_{2_c} = \left[\frac{3}{2}(s_{r_c}^2 + s_{t_c}^2 + s_{z_c}^2) \right]^{1/2} = \sqrt{3}(s_c^2 + \frac{3}{4} s_{z_c}^2)^{1/2} \qquad (7.35)$$

where μ may be called the radiation hardening coefficient or parameter which depends mainly on yield condition, irradiation temperature and creep strain rate of the irradiated cladding material. In general, this parameter is determined experimentally for each particular material and each particular range of irradiation temperatures. For the analysis under consideration, however, μ will be determined by means of a simplified semi-analytical process in a more flexible manner.

It may be recalled from experience in the stress analysis of circular cylinders that the magnitude of radial stress is usually small compared to that of either tangential or axial stress. Particularly, in this case, the radial stresses on the free surface of the inner and outer cladding vanish. Therefore, in practice, the component of the radial stress in the cladding may be neglected, and Eqs. 7.34, 7.35 may be simplified.

$$\begin{aligned} 3(\epsilon_{r_c} - \alpha_c\theta_c) &= \mu(-\sigma_{t_c} - \sigma_{z_c}) \\ 3(\epsilon_{t_c} - \alpha_c\theta_c) &= \mu(2\sigma_{t_c} - \sigma_{z_c}) \\ 3(\epsilon_{z_c} - \alpha_c\theta_c) &= \mu(2\sigma_{z_c} - \sigma_{t_c}) \end{aligned} \qquad (7.34a)$$

$$J_{2_c} = (\sigma_{t_c}^2 - \sigma_{t_c}\sigma_{z_c} + \sigma_{z_c}^2)^{1/2} \qquad (7.35a)$$

Now, solving the first two and the last two equations of Eqs. 7.34a simultaneously for $\mu\sigma_{t_c}$ and σ_{z_c}, it yields

$$\mu\sigma_{t_c} = \varepsilon_{t_c} - \varepsilon_{r_c} = 2\varepsilon_{t_c} + \varepsilon_{z_c} - 3\alpha_c\theta_c \tag{7.36}$$

$$\varepsilon_{r_c} + \varepsilon_{t_c} + \varepsilon_{z_c} - 3\alpha_c\theta_c = 0 \tag{7.37}$$

$$\begin{aligned} \sigma_{z_c} &= p\sigma_{t_c} \\ p &= (2\varepsilon_{z_c} + \varepsilon_{t_c} - 3\alpha_c\theta_c)/(2\varepsilon_{t_c} + \varepsilon_z - 3\alpha_c\theta_c) \end{aligned} \tag{7.38}$$

Eq. 7.37 is, for the cladding, the compatibility equation which imposes the necessary restriction on the components of strains ε_{r_c}, ε_{t_c}, ε_{z_c} and $\alpha_c\theta_c$ of the cladding. Of these ε_{z_c}, $\alpha_c\theta_c$ are constant, ε_{r_c} and ε_{t_c} are respectively given by Eqs. 7.14a and 7.15a at $x = x_i$ or $x = 1$.

By substituting Eq. 7.37 into Eq. 7.35a, the simplified Mises yield criterion for the cladding material becomes

$$J_{2_c} = (1 - p + p^2)^{1/2}\, \sigma_{t_c} \tag{7.39}$$

in which J_{2_c} may be assumed as a known value when the cladding material is given.

Since σ_{t_c}, σ_{z_c} and μ can not be determined explicitly from Eqs. 7.34a alone, it is necessary to use Eqs. 7.36 through 7.39 to obtain their values consistently by appropriate adjustment when the value of J_{2_c} is given.

Once the value of σ_{t_c} is determined, $(\sigma_{t_i})_c$ as well as

$(\sigma_{t_i})_f$ can also be found. This is the crucial process to determine the creep stresses of the fuel element. The value of $(\sigma_{t_i})_c$ which satisfies Eqs. 7.36 and 7.39 at $x = x_i$ is then introduced into Eqs. 7.32 and 7.38, hence

$$\sigma_{r_i} = h_i(\sigma_{t_i})_c/r_0 x_i \tag{7.32a}$$

$$(\sigma_{z_i})_c = p(\sigma_{t_i})_c \tag{7.38a}$$

Similarly, the value of σ_{t_c} at the outer radius of the fuel zone $x = 1$ or $(\sigma_{t_0})_c$ which also satisfies Eqs. 7.36 and 7.39 is used with Eqs. 7.33 and 7.38, respectively, hence

$$\sigma_{r_0} = - h_0(\sigma_{t_0})_c/r_0 \tag{7.33a}$$

$$(\sigma_z)_c = p(\sigma_t)_c \text{ at } x = 1 \tag{7.38b}$$

In common practice, the thicknesses of the inner and outer cladding of fuel elements are equal, $h_i = h_0 = h$. Therefore, Eqs. 7.32a and 7.33a are simply reduced to

$$\sigma_{r_i} = h(\sigma_{t_i})_c/r_0 x_i \tag{7.32b}$$

$$\sigma_{r_0} = - h(\sigma_{t_0})_c/r_0 \tag{7.33b}$$

When the value of σ_{r_i} given by Eq. 7.32a or 7.32b, is substituted into the second of Eqs. 7.26 therefrom, with the aid of Eqs. 7.23 and 7.27, the radial stress distribution in the fuel zone can be obtained. Subsequently, the tangential and

axial stress distribution in the fuel zone can be found from Eqs. 7.28 and 7.29.

As a result, the creep stress distribution in the fuel element is completely determined. Finally, since there is no external force acting on the end surface of the fuel element, the resultant of the axial forces over the cross section must vanish. Hence

$$\int_{x_i}^{1} \sigma_z x dx + (\sigma_{z_c})_i x_i h_i + (\sigma_{z_c})_0 \, 1 \, h_0 = 0 \qquad (7.40)$$

in which the common factor $2\pi r_0$ has been omitted.

To evaluate these three terms on the left side of Eq. 7.40, Eqs. 7.25, 7.29, 7.32, 7.33 and 7.36 are used. Hence

$$\int_{x_i}^{1} \sigma_z x dx = \frac{3}{2} \int_{x_i}^{1} s_z x dx + \int_{x_i}^{1} (\sigma_r - s) x dx$$

$$-s = \frac{1}{2}(\sigma_t - \sigma_r) = \frac{1}{2} x \frac{d\sigma_r}{dx}, \quad \sigma_r - s = \frac{1}{2x} \frac{d(x^2\sigma_r)}{dx}$$

$$\int_{x_i}^{1} (\sigma_r - s) x dx = \frac{1}{2} \int_{x_i}^{1} \frac{1}{x} \frac{d(x^2\sigma_r)}{dx} = \frac{1}{2}\left[\sigma_{r_0} - x_i^2 \sigma_{r_i} \right]$$

$$(\sigma_{z_i})_c x_i h_i - \frac{1}{2} x_i^2 \sigma_{r_i} = \frac{3}{2} \frac{\epsilon_z - \alpha_c \theta_{c_i}}{(2\epsilon_{t_i} + \epsilon_z - 3\alpha_c \theta_{c_i})} x_i^2 \sigma_{r_i}$$

$$(\sigma_{z_0})_c \, 1 \, h_0 + \frac{1}{2} \sigma_{r_0} = \frac{3}{2} \frac{\epsilon_z - \alpha_c \theta_{c_0}}{2\epsilon_{t_0} + \epsilon_z - 3\alpha_c \theta_{c_0}} \sigma_{r_0}$$

Substitution of these and the last of Eq. 7.21 into Eq. 7.40

yields

$$\int_{x_i}^{1} \frac{\epsilon_z - \epsilon_R}{\lambda} x\,dx + \frac{\epsilon_z - \alpha_c\theta_{c_i}}{2\epsilon_{t_i} + \epsilon_z - 3\alpha_c\theta_{c_i}} x_i^2\sigma_{r_i}$$

$$- \frac{\epsilon_z - \alpha_c\theta_{c_0}}{2\epsilon_{t_0} + \epsilon_z - 3\alpha_c\theta_{c_0}} \sigma_{r_0} = 0 \qquad (7.40a)$$

where ϵ_{t_i}, ϵ_{t_0} = tangential strains of the inner and outer cladding at $x = x_i$ and $x = 1$ respectively

θ_{c_i}, θ_{c_0} = effective temperatures of the inner and outer cladding at $x = x_i$ and $x = 1$ respectively

Eq. 7.40a can be used to check the results of calculation if the resultant of the axial forces over the cross section of the fuel element vanishes closely.

E. The State of Plane Strain

In most practical cases, cylindrical fuel elements are used for power reactors. The mean radius of the fuel element is usually much greater than its thickness, and, in turn, the length of the fuel element is much greater than its mean radius. If the end sections of the fuel elements in each fuel assembly are so confined that displacement in the axial direction is prevented. Thus there will be no axial displacement at the ends and, by symmetry, at the mid-section of the fuel

element. This situation may be generalized that the same holds at every cross section of the long fuel element. Therefore, in such case, the stress analysis for the fuel element may be simplified and considered as a plane strain problem in which the axial strain, ϵ_z, is zero.

Furthermore, in applying the Saint-Venant principle to the long fuel element, stress distribution at cross sections that are distant, compared to the mean radius, from the ends of the fuel element is practically uniform. Therefore, the stress and strain equations derived above are justified and valid for the fuel element under consideration.

Based on the plane strain problem and the Saint-Venant principle discussed above, Eqs. 7.10a, 7.14, 7.15, 7.16, 7.24, 7.36 and so on automatically reduce to

$$\epsilon_r + \epsilon_t - \epsilon_R = 0 \tag{7.10b}$$

$$\epsilon_t = \frac{u}{x} = \frac{1}{x^2}\left[\epsilon_{t_0} - 3 \int_x^1 \epsilon_R x dx \right] \qquad x_i \le x \le 1 \tag{7.14a}$$

$$\epsilon_r = \frac{\partial u}{\partial x} = \frac{1}{x^2}\left[-\epsilon_{t_0} + 3 \int_x^1 \epsilon_R x dx - 3x \frac{\partial}{\partial x} \int_x^1 \epsilon_R x dx \right]$$

$$x_i \le x \le 1 \tag{7.15a}$$

$$\epsilon = \frac{1}{x^2}\left[-\epsilon_{t_0} + 3 \int_x^1 \epsilon_R x dx - \frac{3x}{2} \frac{\partial}{\partial x} \int_x^1 \epsilon_R x dx \right] \qquad x_1 \le x \le 1 \tag{7.16a}$$

$$\lambda = \frac{\sqrt{3}}{J_2}\left[\epsilon^2 + \frac{3}{4} \epsilon_R^2 \right] \qquad (7.24a)$$

$$\mu = (2\epsilon_t - 3\alpha_c\theta_c)/\sigma_{t_c} \text{ , etc.} \qquad (7.36a)$$

F. Calculations for Creep Strains and Stresses of the Fuel Element

In the state of plane strain, we begin with the relations for the resultant linear thermal and radiation dilatation, ϵ_R

$$\epsilon_R = \alpha\,\theta + \epsilon_I \qquad (7.11a)$$

where α = linear coefficient of thermal expansion of the fuel material

θ = effective radial temperature distribution in the fuel material

ϵ_I = linear strain due to thermal-cycling growth, irradiation growth and swelling

as defined previously. Within the range of a moderate change in temperature, α may be assumed as a constant. The value of θ is given by Eq. 6.4 or 6.12. For simplicity and practical consideration, the value of θ given by Eq. 6.4a or 6.12a is advantageous to use where the experimental, approximate solution for the neutron flux distribution has been utilized. Since both thermal-cycling and irradiation growth coefficients, G_t and G_i, are exponential functions in characteristics;

for moderate thermal-cycling growth, irradiation growth and swelling, ϵ_I, in the fuel element it may be assumed that

$$\epsilon_I = \epsilon_{I_0} e^{x_m - x} \qquad x_l \leq x \leq x_m$$
$$\epsilon_I = \epsilon_{I_0} e^{x - x_m} \qquad x_m \leq x \leq 1 \tag{7.41}$$

where ϵ_{I_0} = linear thermal-cycling and radiation dilatation at x_m of the fuel element

$x_m = r_m/r_0$, and r_m = mean radius of the fuel element

Now, by using Eqs. 6.4a, 6.12a and 6.22 the effective radial temperature distribution, θ, will be given by Eq. 6.24 or 6.25. Further, by applying the strain and stress equations derived above, the creep strains and stresses of the fuel element can be calculated when the properties of materials and the strain parameters are given.

The procedure to calculate the components of creep strain and stress for the fuel element under consideration is as follows:

1. Calculation for the components of creep strain ϵ_t, ϵ_r and ϵ

In order to calculate these components of the creep strain for a known or assumed temperature on the inner surface of the fuel zone, θ_{r_i}, Eqs. 6.24, 7.11a, 7.14a through 7.16a

are used. Hence (see Appendix B)

$$\epsilon_t = \frac{\epsilon_{t_0}}{x^2} - \frac{3\alpha}{2x^2}(1 - x^2)\theta_{r_i} - \frac{3a\alpha\beta}{4kx^2} M_1\Big[- \frac{1}{2}(1 - x^2) - \ln x_i$$

$$- x^2 \ln \frac{x}{x_i} \Big] + \frac{3a\alpha}{4kx^2}\Big[(1 + br_0^2c^2)x_i^2\{\frac{1}{4x_i^2}(1 - x^4)$$

$$+ \frac{1}{2}(1 - x^2) + \ln x_i + x^2 \ln \frac{x}{x_i}\} + br_0^2\{(\frac{1}{24}(1 - x^6) \qquad (7.42)$$

$$- \frac{8c}{45}(1 - x^5) - x_i^3(\frac{x_i}{2} - \frac{4c}{3})(\frac{x^2}{2} - \frac{1}{2} - \ln x_i - x^2 \ln \frac{x}{x_i})\}$$

$$- M_2(1 - x^2) \Big] + \frac{3}{x^2} \epsilon_{I_0} e^{|x - x_m|}(1 - x) \qquad x_i \le x \le 1$$

$$\epsilon_r = - \frac{\epsilon_{t_0}}{x^2} + \frac{3\alpha}{2x^2}(1 + x^2)\theta_{r_i} + \frac{3a\alpha\beta M_1}{4kx^2}\Big[\frac{1}{2}(x^2 - 1) - \ln x_i$$

$$+ x^2 \ln \frac{x}{x_i} \Big] - \frac{3a\alpha}{4kx^2}\Big[(1 + br_0^2c^2)x_i^2\{\frac{1}{4x_i^2}(1 + 3x^4) - \frac{x^2}{2}$$

$$+ \frac{1}{2} + \ln x_i - x^2 \ln \frac{x}{x_i}\} + br_0^2\{\frac{1}{24}(1 + 5x^6) - \frac{8c}{45}(1 + 4x^5)$$

$$- x_i^3(\frac{x_i}{2} - \frac{4c}{3})(\frac{x^2}{2} - \frac{1}{2} - \ln x_i - 3x^2 \ln \frac{x}{x_i})\} - M_2(1 + x^2) \Big]$$

$$+ \frac{3}{x^2} \epsilon_{I_0} e^{|x - x_m|}(1 - x + x^2) \qquad x_i \le x \le 1 \qquad (7.43)$$

$$\varepsilon = \frac{1}{2}(\varepsilon_r - \varepsilon_t)$$

$$= -\frac{\varepsilon_{t_0}}{x^2} + \frac{3\alpha}{2x^2}\theta_{r_i} + \frac{3a\alpha\beta M_1}{4kx^2}\left[\frac{1}{2}(x^2 - 1) - \ln x_i\right]$$

$$- \frac{3a\alpha}{4kx^2}\Big[(1 + br_0^2c^2)x_i\{\frac{1}{4x_i^2}(1 + x^4) - \frac{x^2}{2} + \frac{1}{2} + \ln x_i\}$$

$$+ br_0^2\{\frac{1}{24}(1 + 2x^6) - \frac{8c}{45}(1 + \frac{3}{2}x^5) - x_i^3(\frac{x_i}{2} - \frac{c}{3})(\frac{x^2}{2} - \frac{1}{2}$$

$$- \ln x_i - 2x^2 \ln \frac{x}{x_i})\} - M_2\Big] + \frac{3}{x^2}\varepsilon_{I_0} e^{|x - x_m|}(1 - x + \frac{x^2}{2})$$

$$x_i \leq x \leq 1 \qquad (7.44)$$

where ε_{t_0}, ε_{I_0}, θ_{r_i}, α, β and k, as defined before, are respectively the numerical and material parameters, a, b and c are constants, M_1 and M_2 are given by the first two of Eqs. 6.27 and, referring to Eq. 7.41,

$$e^{|x - x_m|} = e^{x_m - x} \qquad \text{for } x_i \leq x \leq x_m$$

$$e^{|x - x_m|} = e^{x - x_m} \qquad \text{for } x_m \leq x \leq 1$$

In order to determine the constants a_0, b and c_0 in Eq. 6.21 or a, b and c in Eq. 6.22, the self-shielding effect of fuel material is taken into account. With the thermal neutron flux distribution as shown in Fig. 4b, the magnitude of the

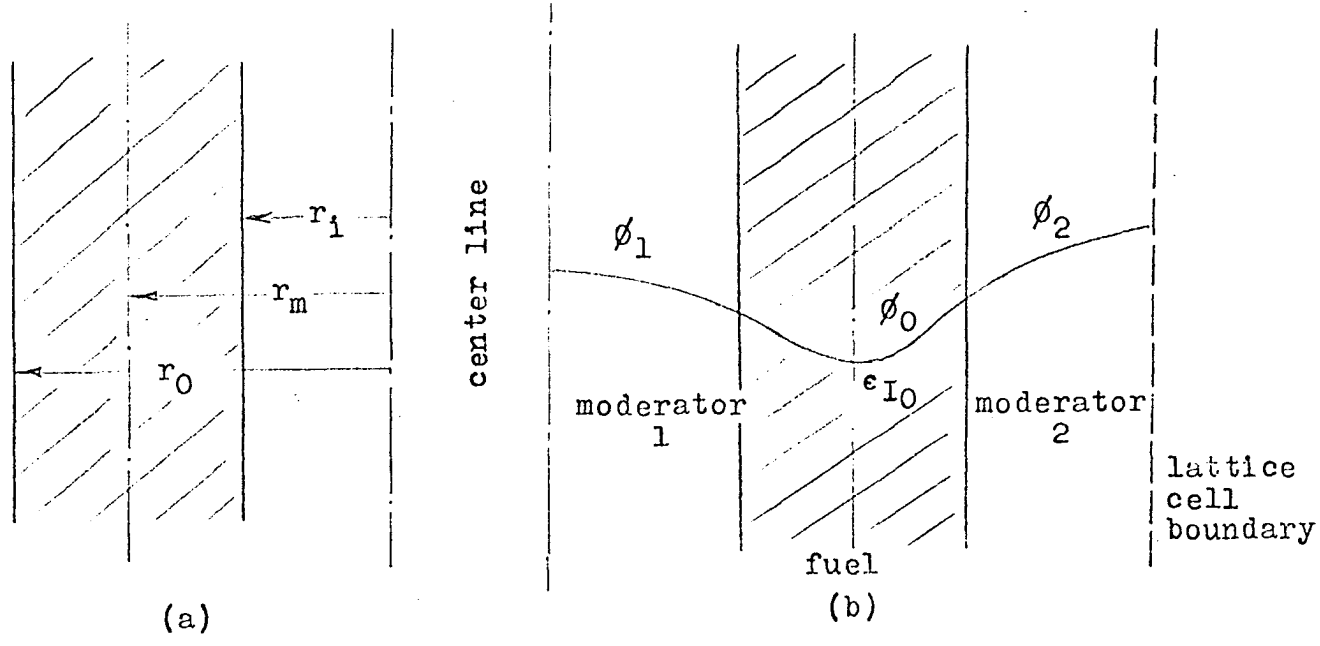

Fig. 4. Thermal neutron flux distribution in fuel and moderators

flux, in neutrons per cm^2 per sec, at the inner, mean and outer radii of the fuel zone may be approximately assumed below:

$$\begin{aligned} \phi_0 &= 4(10^{10}) \quad \text{for} \quad r = r_i \quad \text{or} \quad x = x_i \\ \phi_0 &= 5(10^{9}) \quad \text{for} \quad r = r_m \quad \text{or} \quad x = x_m \\ \phi_0 &= 5(10^{10}) \quad \text{for} \quad r = r_0 \quad \text{or} \quad x = 1 \end{aligned} \tag{7.45}$$

By substituting these values into Eq. 6.21 and solving for the constants, it gives

$$a_0 = \frac{5(10^{10})}{1 + br_0^2(1 - c)^2} = \frac{4(10^{10})}{1 + br_0^2(x_i - c)^2}$$

$$b = -\frac{1}{r_0^2[\,5(x_i-c)^2 - 4(1-c)^2\,]} = -\frac{7}{r_0^2[\,8(x_m-c)^2 - (x_i-c)^2\,]} \tag{7.46}$$

$$c = \frac{c_0}{r_0} = (2x_m^2 - 9x_i^2 + 7)/(4x_m - 18x_i + 14)$$

If Eqs. 7.46 are introduced into Eqs. 6.21, 6.22, 6.23, 7.42, 7.43 and 7.44, the neutron flux distribution ϕ_0, the volumetric heat generation rate q_v and the components of creep strain ϵ_t, ϵ_r and ϵ can be readily found.

2. Calculation of the radiation hardening coefficient μ and the tangential stress σ_{t_c} for cladding material

For a given cladding material the linear coefficient of thermal expansion, α_c, corresponding to the mean temperature, θ_c, is known. The tangential strain ϵ_{t_c} of the cladding, with aid of the second of Eqs. 7.30 or 7.31, can be obtained from Eq. 7.42, step 1 above. By substituting these values into Eqs. 7.36 and 7.39, μ and σ_{t_c} $(= \sigma_{t_f})$ either at $x = x_i$ or at $x = 1$ can be found after the values of J_{2_c} has been assumed or obtained experimentally.

3. Calculation of the parameter λ and the second stress invariant J_2 for fuel material

For a given fuel material, its linear coefficient of thermal expansion, α, corresponding the mean fuel temperature, is approximately a constant. By using Eqs. 6.4a and 7.11a the resultant linear thermal and radiation dilatation becomes

$$\epsilon_R = \alpha\theta_{r_i} + \frac{a\alpha\beta M_1}{2k} \ln\frac{x}{x_i} - \frac{a\alpha}{2k}\Big[(1 + br_0^2c^2)\left(\frac{x}{2} - x_i^2 \ln\frac{x}{x_i}\right)$$

$$+ br_0^2\left\{x^3\left(\frac{x}{8} - \frac{4c}{9}\right) - x_i^3\left(\frac{x_i}{2} - \frac{4c}{9}\right)\ln\frac{x}{x_i}\right\} - M_2\Big]$$

$$+ \epsilon_{I_0} e^{|x - x_m|} \qquad (7.47)$$

in which β, M_1, M_2, ϵ_{I_0}, a, b and c have been defined before (see step 1). Introduction of this and Eq. 7.44 into Eq. 7.24a yields the results for the determination of the parame-

ter λ when J_2 has been known or assumed. In general, J_2 or the yield strength of fuel material under consideration can be found experimentally from a simple shear test.

4. Calculation for the components of creep stress σ_r, σ_t and σ_z

First, by using Eqs. 7.27, 7.32 and 7.33 the radial stress σ_{r_i} at $x = x_i$ or σ_{r_0} at $x = 1$ of the fuel zone can be determined when σ_{t_c} at $x = x_i$ or $x = 1$ has been found. Substitution of either σ_{r_i} or σ_{r_0} into Eqs. 7.26 respectively with the aid of Eqs. 7.23 and 7.44, after performing the integration between appropriate limits, yields the radial stress distribution in the fuel zone. For example, by introducing the first of Eqs. 7.23 and Eq. 7.44 into the second of Eqs. 7.26 and integrating between $x = x_i$ and any point x, the resulting equation for the radial stress distribution in the fuel zone is obtained.

$$\sigma_r = \sigma_{r_i} - \frac{2}{\lambda}\left[\frac{1}{2}\epsilon_{t_0}\left(\frac{1}{x^2} - \frac{1}{x_i^2}\right) - \frac{3\alpha}{4}\left(\frac{1}{x^2} - \frac{1}{x_i^2}\right)\theta_{r_i}\right.$$

$$+ \frac{3a\alpha\beta M_1}{4k}\left[\frac{1}{4}\left(\frac{1}{x^2} - \frac{1}{x_i^2}\right)(1 + 2\ln x_i) + \frac{1}{2}\ln\frac{x}{x_i}\right]$$

$$- \frac{3a\alpha}{4k}\left[(1 + br_0^2c^2)x_i^2\left\{-\frac{1}{4}\left(\frac{1}{2x_i^2} + 1 + 2\ln x_i\right)\left(\frac{1}{x^2} - \frac{1}{x_i^2}\right)\right.\right.$$

$$+ \frac{1}{8x_i^2}(x^2 - x_i^2)\} + br_0^2\{-(\frac{1}{48} - \frac{4c}{45})(\frac{1}{x^2} - \frac{1}{x_i^2}) + \frac{1}{48}(x^4 - x_i^4)$$

$$- \frac{4c}{45}(x^3 - x_i^3) - x_i^3(\frac{x_i}{2} - \frac{4c}{4})\Big[(\frac{1}{2} + 2 \ln x_i)\ln \frac{x}{x_i}$$

$$+ \frac{1}{2}(\frac{1}{2} + \ln x_i)(\frac{1}{x^2} - \frac{1}{x_i^2}) - (\ln x)^2 + (\ln x_i)^2\Big]\}$$

$$+ \frac{1}{2} M_2(\frac{1}{x^2} - \frac{1}{x_i^2})\Big] + \frac{3}{2} \epsilon I_0 e^{|x - x_m|}(\frac{1}{x} - \frac{1}{x^2} - \frac{1}{x_i} e^{x_i - x}$$

$$+ \frac{1}{x_i^2} e^{x_i - x})\Big] \qquad (7.48)$$

in which the parameter λ has been determined from step 3 above.

Next, by substituting Eqs. 7.42, 7.43, 7.44, 7.47 and the values of λ obtained above into Eqs. 7.22 and 7.23 respectively, thus s_r, s_t, s_z and s are found.

Finally, introduction of the values of s and s_z into Eqs. 7.28 and 7.29 yields the tangential and axial stress distributions in the fuel zone.

Of the creep stress distribution determined above these three components which represent the principal stress distribution developed in the fuel zone due to the thermal and radiation effects have great influence on the mechanical stability

of the fuel elements used in nuclear reactors.

Here it may be also noted from Eqs. 7.23 that in the particular case when $\lambda = 1$, the effective stress $\sigma = s$ numerically.

5. Calculation for the components of creep strain and stress of cladding material

From the boundary conditions of strain, Eqs. 7.30 and 7.31, the components of creep strain ϵ_{r_c}, ϵ_{t_c} and ϵ_{z_c} can be readily found when ϵ_r, ϵ_t and ϵ_z, if any, at $x = x_i$ and $x = 1$ have been evaluated from Eqs. 7.10a, 7.42 and 7.43 respectively. These results obtained must satisfy the conditions of compatibility and incompressibility for both fuel and cladding materials of the fuel elements.

At the same time, by using Eqs. 7.34 and 7.38, σ_{r_c}, σ_{t_c}, σ_{z_c}, s_r, s_t, s_z and s at $x = x_i$ and $x = 1$ can be determined. These results may be checked with those obtained from the preceding step for fuel material.

6. Finally, Eq. 7.40a is used to check if the resultant of the axial forces over the cross section of the fuel element vanishes. Otherwise, the procedure outlined above must be repeated until Eq. 7.40a is satisfied. Experience shows that cladding thickness h (or h_i, h_o), cladding mean temperature θ_c and so on need to be adjusted properly in order to render Eq. 7.40a practically zero.

Here it may be mentioned that the application of the membrane theory to thin cladding of the fuel element has simplified the calculations in steps 5 and 6 appreciably.

In order to apply these equations derived for the components of creep strain and stress and to illustrate the use of the procedure outlined above, the following example is chosen. Let

(a) Fuel material (uranium alloy)

$x_i = 0.6$ $\qquad$ $x_m = 0.8$

$\sigma_f = 580\ (10^{-24})\ cm^2$ $\qquad$ $\rho = 18.6\ gm/cm^3$

$\phi = 5\ (10^{10}),\ 5\ (10^{11})$ neutrons/cm^2-sec at $x = 1$

$E_f = 200$ Mev/fission

$\theta_{r_i} = 450°F,\ 550°F,\ 650°F$ at $x = x_i$

$\alpha = 12\ (10^{-6})$ in/in-F

$k = 18.8$ Btu/ft-hr-F (29)

$= 1.56$ Btu/in-hr-F

$J_2 = 3{,}000$ psi for $\theta_{r_i} = 550 - 650°F$

(b) Cladding material (zircaloy-2)

$\theta_c = 500°F,\ 600°F$

$\alpha_c = 12\ (10^{-6})$ in/in-F

$k_c = 6.5$ Btu/ft-hr-F

$= 0.55$ Btu/in-hr-F

$h/r_0 = h_i/r_0 = h_0/r_0 = 0.03$

$J_{2_c} = 17{,}500$ psi for $\theta_c = 500 - 600°F$

(c) Strain parameters

ϵ_{t_0} = 0.005, 0.01, 0.02, 0.03 in/in

ϵ_{I_0} = 0.005, 0.01 in/in

(d) Fraction of heat transferred from inner passage of coolant

β = 0.50, 0.40, 0.30

Following the procedure outlined above the numerical calculations are made below.

1. Upon substitution of the values for σ_f, ρ, E_f, x_i, x_m, θ_{r_i}, α, β, k, ϵ_{t_0} and ϵ_{I_0} into Eqs. 6.21, 6.23, 6.27, 7.42, 7.43, 7.44 and 7.46 respectively, the constants a_0, a, b, c, M_1 and M_2 are determined and the components of creep strain ϵ_t, ϵ_r as well as ϵ are calculated. The values of these constants obtained are given below:

$a_0 = 3.9947\ (10^{11})$ neutrons/cm^2-sec

$a = 2.2050\ (10^{16})$ Mev/cm^3-sec

$= 3.4177\ (10^8)$ Btu/ft^3-hr

$= 1.9778\ (10^5)$ Btu/in^3-hr

$b = 23.60827/r_0^2$ $\qquad$ $c = 0.6075$

$M_1 = 1.49840$ $\qquad$ $M_2 = 0.75394$

The results calculated for ϵ_t, ϵ_r and ϵ are respectively given in Tables 1, 2 and 3, Appendix B. From Table 1, for the given thickness of the fuel zone, the distribution of tangential strain ϵ_t varying with the fractions of total heat

transferred per unit length of the fuel by the inner passage of coolant is shown in Fig. 5. Similarly, the variations of tangential strain in the fuel zone with the values of ϵ_{I_0} = 0.005, 0.010 and with the values of θ_{r_i} = 450°F, 550°F, 650°F are respectively shown in Figs. 6 and 7. From Table 2, the variation of radial strain in the fuel zone with the various values of ϵ_{t_0} is shown in Fig. 8. For purposes of comparison, the components of creep strains ϵ_t, ϵ_r of non-irradiated material are also shown in Figs. 6, 7 and 8 respectively.

2. By using the second of Eqs. 7.30, $(\epsilon_{t_i})_f = (\epsilon_{t_i})_c$ at $x = x_i$, the values of $(\epsilon_{t_i})_c$ for the inner cladding are obtained from the preceding step. Substitution of those calculated values of $(\epsilon_{t_i})_c$ and those given values of α_c and θ_c into Eqs. 7.36, 7.38 and 7.39 results in the necessary relations to determine the radiation hardening coefficient μ and the tangential stress $(\sigma_{t_i})_c$ when the second stress invariant J_{2_c} for cladding material is known. For the zirconium alloy, zircaloy-2, within the working temperature range 450° to 750°F, the yield strength is about 42,000 psi (30) and the creep strength with 15% cold worked conditions is between 10,000 and 22,000 psi (31). On the basis of these experimental data of zircaloy-2, it appears appropriate to take the value J_{2_c} = 17,500 psi so that from Eq. 7.39 it is found $(\sigma_{t_i})_c$ = 20,000 psi for θ_c = 500 - 600°F.

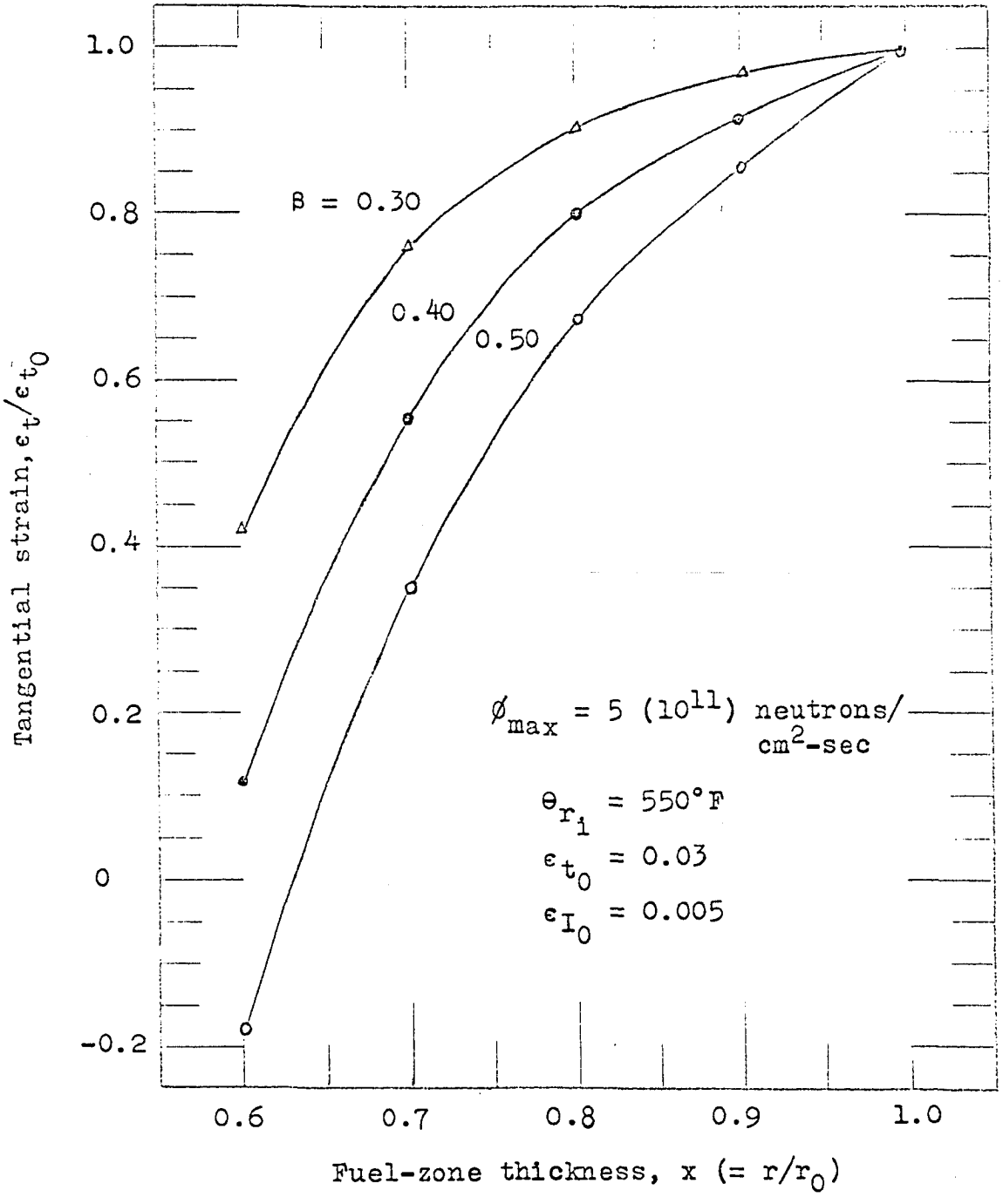

Fig. 5. Tangential strain varies with the fractions of total heat transferred per unit length of fuel element by the inner passage of coolant

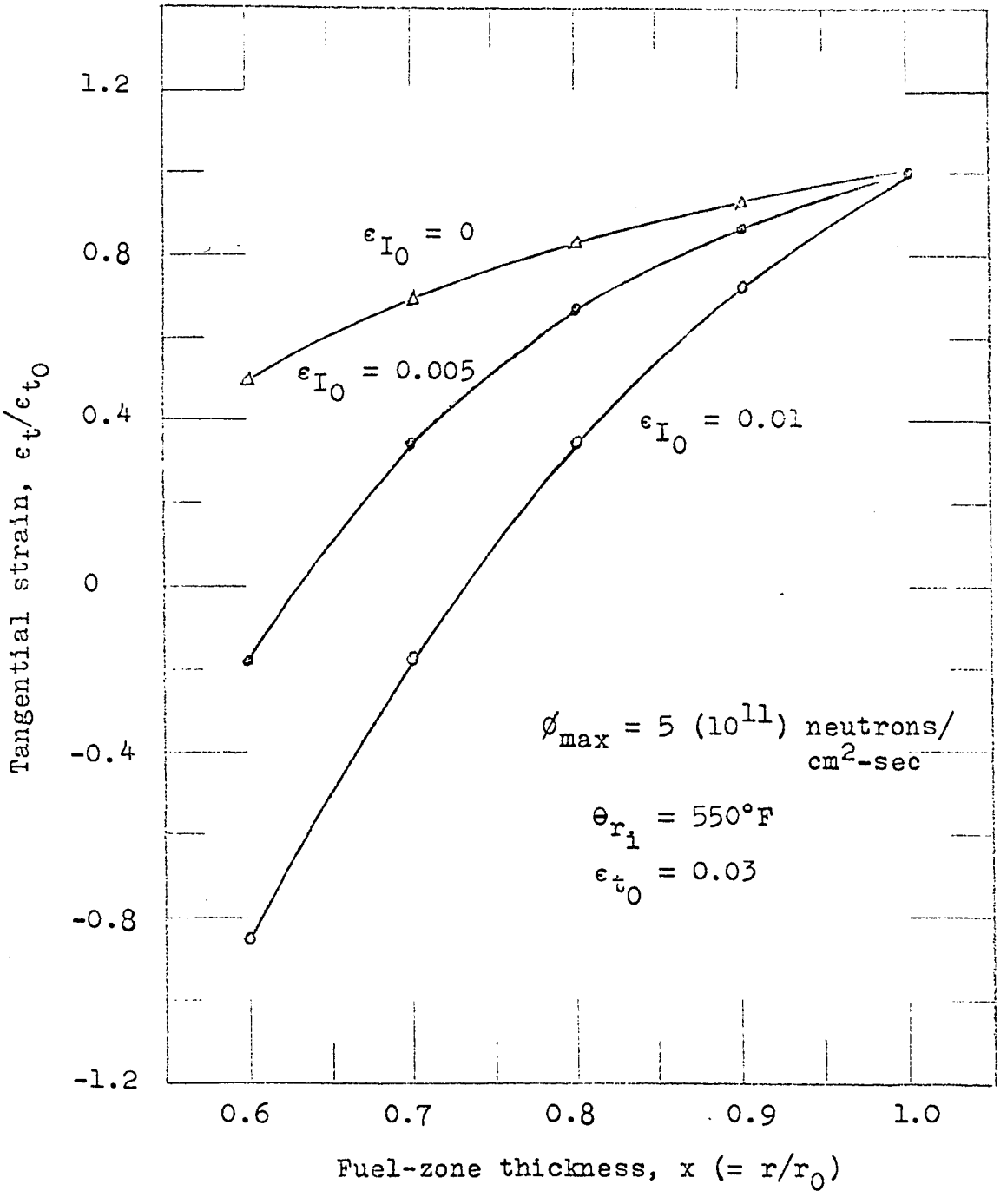

Fig. 6. Tangential strain varies with the various values of linear thermal cycling and radiation dilatation

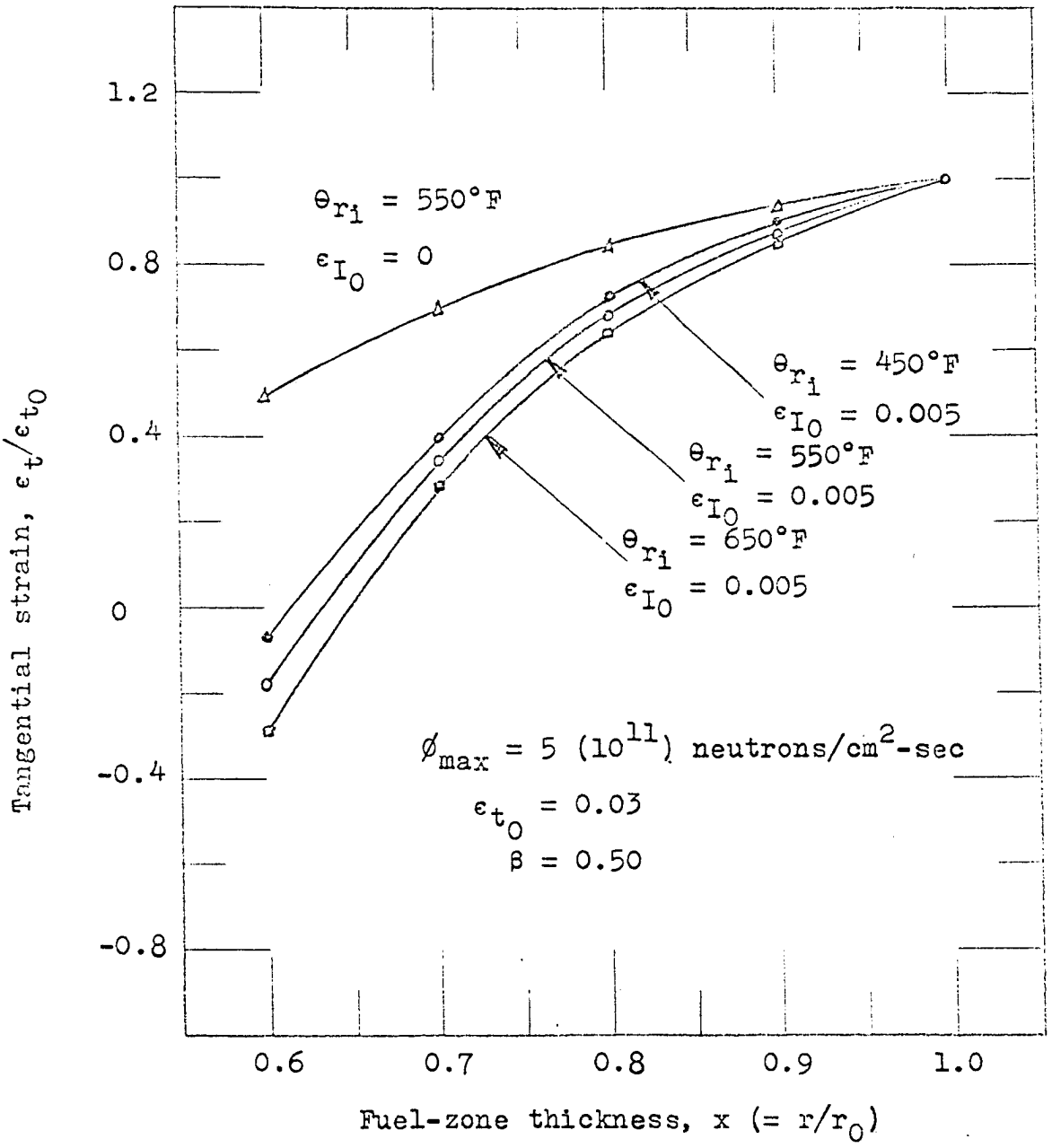

Fig. 7. Variation of tangential strains with the temperatures at the inner fuel surface

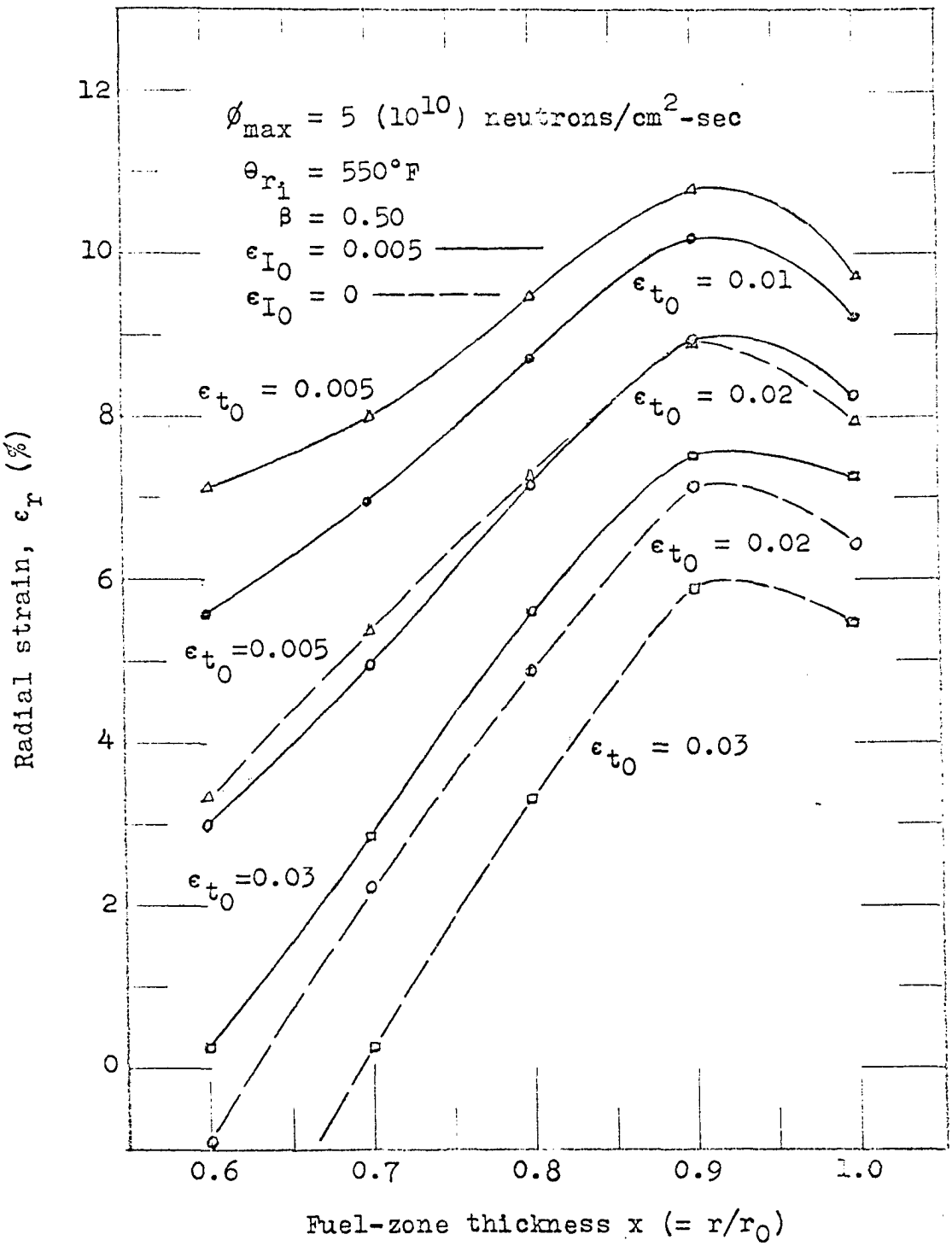

Fig. 8. Radial strain varies with the various tangential strains at the outer surface of the fuel zone

3. With the given values for Θ_{r_i}, x_i, x_m, α, β and the calculated values of a, b, c, M_1 and M_2, from Eq. 7.47 the resultant linear thermal and radiation dilatation ϵ_R is computed. The resulting values of ϵ_R for the two different temperatures of Θ_{r_i} and the two different radiation strains of ϵ_{I_0} are given in Table 4, Appendix B, and also shown in Fig. 9. It is seen that ϵ_R increases with ϵ_{I_0} more rapidly than ϵ_R increases with Θ_{r_i}.

By introducing the values ϵ_R and ϵ calculated above into Eq. 7.24a the relation to determine the parameter λ is obtained. For uranium metal at 1000°F, the yield strength is approximately in the neighborhood of 4000-5500 psi (32). Therefore, on the conservative side, the value for J_2 in this case is taken to be J_2 = 3,000 psi. From the above resulting relation of Eq. 7.24a, the numerical values for λ are then determined and given in Table 5, where the condition, $0 \leq \lambda \leq 1$ for $x_i \leq x \leq 1$, is satisfied.

4. By substituting the value of $(\sigma_{t_i})_c$ (= 20,000 psi, compression) obtained from step 2 and the value h_i/r_0 (= 0.03) given above into Eq. 7.32, the radial stress for the inner cladding is found. Furthermore, combination of the second of Eqs. 7.27 and Eq. 7.32 determined the radial stress σ_{r_i} on the inner surface of the fuel zone. In this particular case, σ_{r_i} = - 1,000 psi. Now, use of Eq. 7.48 with the given values

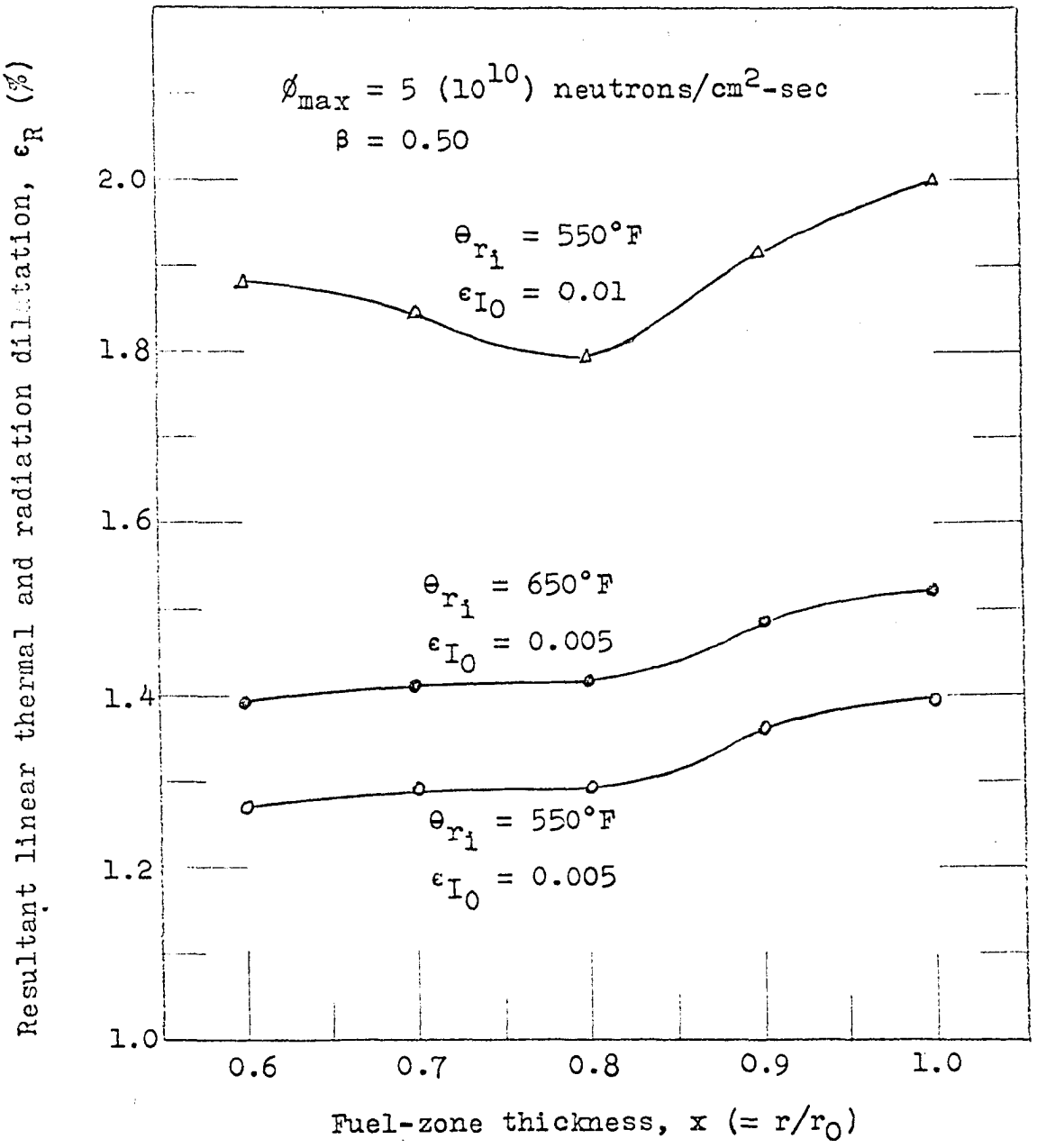

Fig. 9. Resultant thermal and radiation dilatation, ϵ_R, varies with θ_{r_i} and ϵ_{I_0}

of α, β, θ_{r_i}, k, x_i, x_m, ϵ_{t_0}, ϵ_{I_0} and the calculated values of a, b, c, M_1, M_2 and λ yields results for the radial stress distribution in the fuel zone. These radial creep stresses are given in Table 6, Appendix B.

Similarly, by introducing Eq. 7.47 and the value of λ into the last of Eq. 7.22, the axial stress deviation, s_z, is found. In addition, by substituting Eq. 7.44 and the value of λ into the first of Eqs. 7.23, the effective stress, s, is obtained.

Therefore, introduction of the respective values of s and s_z into Eqs. 7.28 and 7.29 yield the tangential and axial stress distributions produced in the fuel zone. The results of these tangential and axial stresses are also given in Table 6. From this table the radial, tangential and axial stress distributions at the three different cases are respectively shown in Figs. 10, 11 and 12. It is seen from this particular problem that the radial, tangential and axial stress distributions for each case are similar in pattern.

5. From the membrane theory of thin cladding and the boundary conditions of strain, Eqs. 7.30 and 7.31, the components of strain, ϵ_{r_c} and ϵ_{t_c} at $x = x_i$ and $x = 1$ are readily obtained because ϵ_r and ϵ_t on the interface of the fuel and cladding materials have been found in step 1. In the state of plane strain under consideration, it requires $\epsilon_{z_f} = \epsilon_{z_c} = 0$ identi-

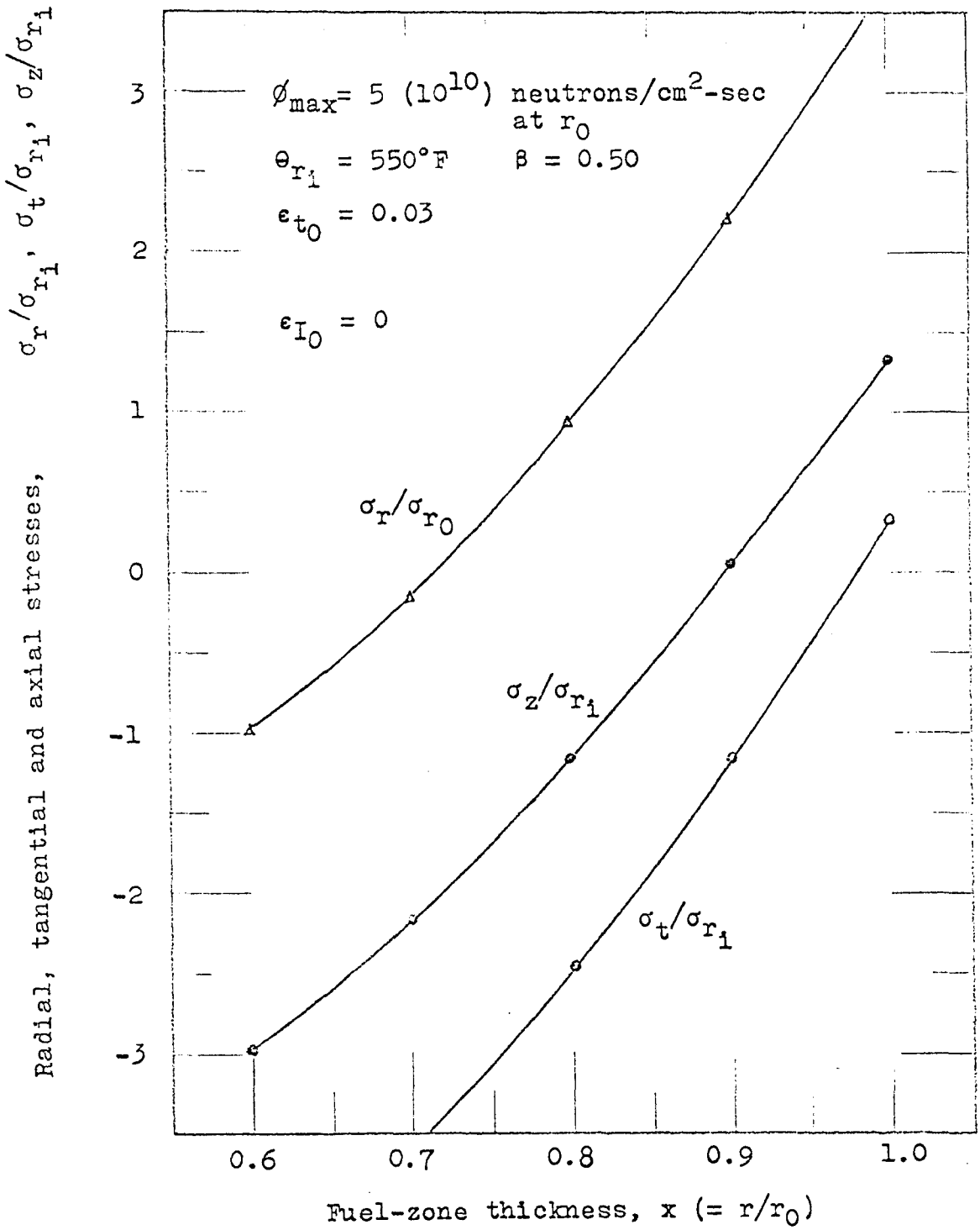

Fig. 10. Stress distribution in fuel zone with $\epsilon_{I_o} = 0$

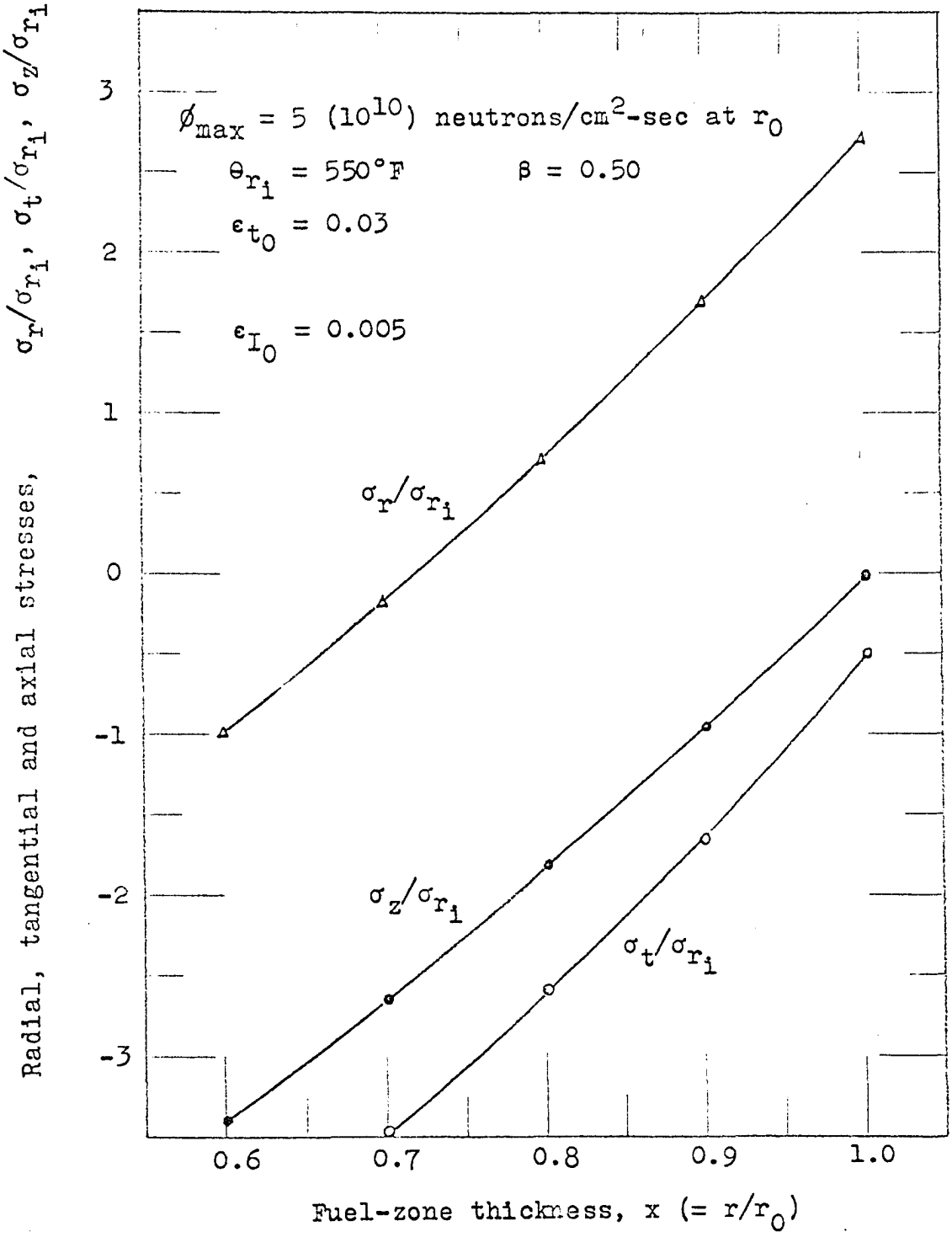

Fig. 11. Stress distribution in fuel zone with ϵ_{I_0} = 0.005

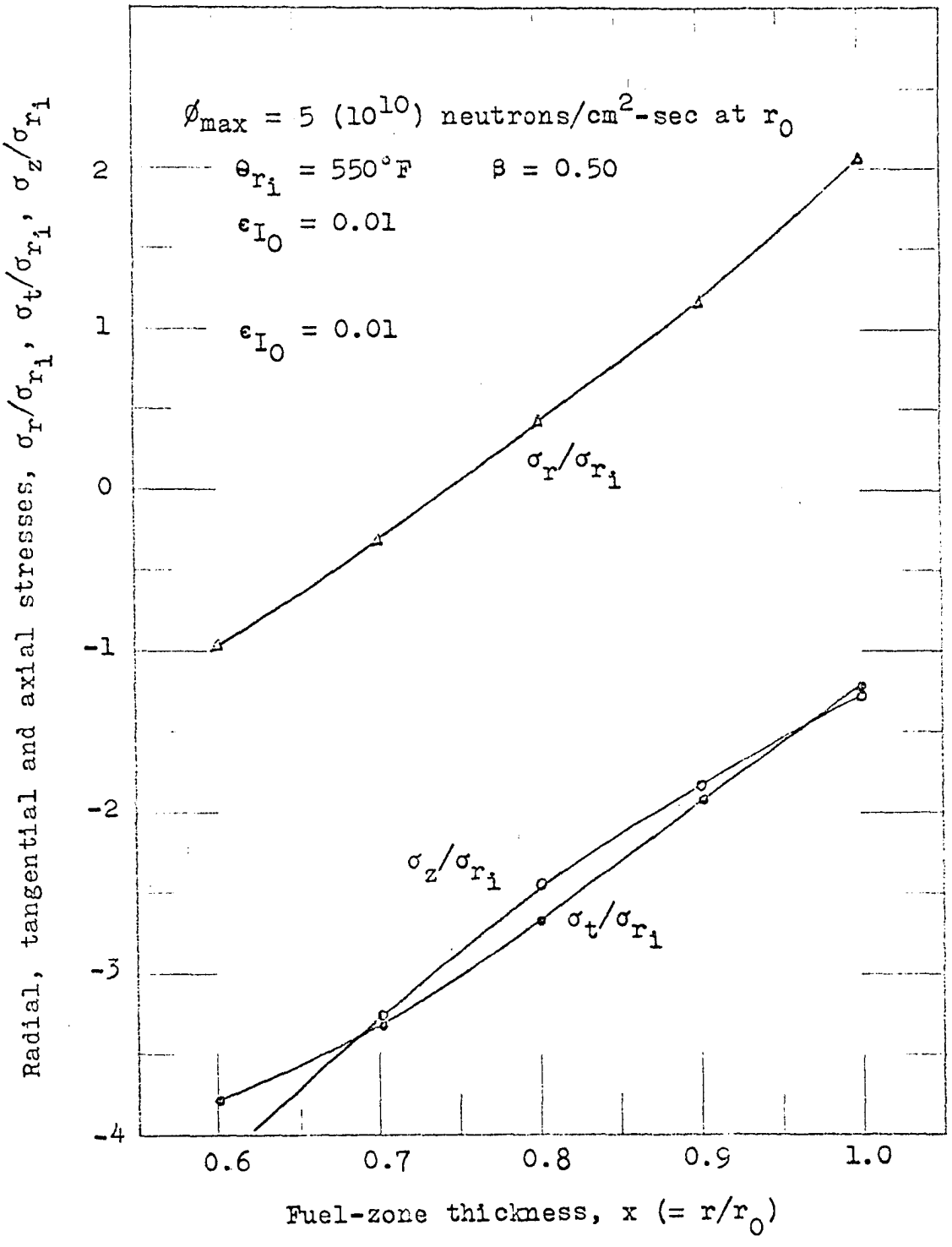

Fig. 12. Stress distribution in fuel zone with ϵ_{I_o} = 0.01

cally.

At the same time, on the basis of the membrane theory and the boundary conditions of stress, Eqs. 7.27, σ_{r_c}, σ_{t_c}, σ_{z_c}, s_r, s_t, s_z and s at $x = x_i$ and $x = 1$ are also readily obtained.

6. Finally, a check for Eq. 7.40a shows that the resultant of the axial forces over the cross section of the fuel element is practically equal to zero.

Results obtained from the calculation of this example reveal several interesting points in regard to the stability of the fuel elements, i.e.

1. The tangential strain, $\epsilon_t/\epsilon_{t_0}$, is the lowest when the amount of heat transferred from internal and external passages of coolant is even, Fig. 5.
2. For a given value of ϵ_{t_0}, the tangential strain produced at the inner surface of the fuel zone increases with ϵ_{I_0} or ϵ_I, Fig. 6. This will cause physical instability of the fuel element.
3. The higher the inner surface temperature θ_{r_i} is, the greater the compressive tangential strain, $\epsilon_t/\epsilon_{t_0}$, at $x = x_i$ will be, Fig. 7.
4. A weaker or thinner outer cladding which may give a relatively large value of ϵ_{t_0} tends to release the radial strain, ϵ_r, on one side, as shown in Fig. 8, while a large stress will be produced in the cladding on the other

side.

5. The resultant linear thermal and radiation dilatation, ϵ_R, increases with θ_{r_i} and ϵ_I, Fig. 9, as expected.
6. For a given value of σ_{r_i}, the components of stress, σ_r, σ_t and σ_z decrease with ϵ_{I_0}, Figs. 10, 11 and 12.
7. The order of magnitude of neutron flux as well as total integrated neutron flux distributed in the fuel is one of the controlling factors to the stability of the fuel element. (Compare Figs. 6 and 8.)

VIII. CONCLUSIONS

From the foregoing realistic study for the stability of cylindrical fuel elements used in nuclear power reactors, the following conclusions may be drawn.

1. Both uranium alloy gamma-phase fuel elements and uranium-compound dispersion fuel elements are of interest and have considerable promise with respect to the demands for greater thermal efficiency and economic operation in the production of nuclear power. Although ceramic fuel elements have recently gained ground, the inherent advantages of metallic fuel elements still hold basic incentives. It is believed that the combination of ceramic and metallic fuel elements which would combine the advantages of both ceramic and metal fuels will become more promising and important in the future development.
2. Both metallic and ceramic fuel elements exhibit, more or less, thermal-cycling growth, irradiation growth and swelling in nuclear power reactors. Fortunately, the thermal-cycling growth which, for a given fuel material, depends only on cycling variables or transient states of the system does not become serious for steadily operating power reactors. The irradiation growth occurs merely at relatively low temperatures and the growth rate falls to zero in the neighborhood of 450°C (8). The irradiation

swelling, however, occurring at relatively high temperatures, great rates and high percentages of burn-up of the fuel material is really one of the serious problems in power-reactor operation, performance and, economics, because there is a continual desire for higher operating temperatures and higher burn-ups in power-producing reactors.

3. Creep of uranium is greatly accelerated by irradiation and presents another serious problem imposed on the successful operation, performance and economics of power reactors. In fact, the thermal and irradiation creep has a direct effect on the stability of the fuel elements in the production of nuclear power. It may be possible that thermal and irradiation creep eventually interact in the nuclear fuel materials.
4. Excessive creep stresses and strains produced in a fuel element are the direct cause for an instability of the fuel element which, in turn, may damage fuel assembly, block the coolant passages and, consequently, affect the operation of the power reactor.
5. The thermal and irradiation creep analysis for the stress as well as the strain distribution in the fuel element given realistically above reveals the primary, interesting facts as follows:

   (a) The principal components of stress, σ_r, σ_t, σ_z in

this particular case, decreases with increasing linear thermal-cycling and radiation dilatation ϵ_{I_0} as shown in Figs. 10, 11 and 12. This is probably due to relief of stresses through the thermal and irradiation creep and increase in tensile strength of the fuel and cladding materials by irradiation.

(b) The principal components of strain, ϵ_r, ϵ_t increase rapidly with the linear thermal-cycling and radiation dilatation ϵ_{I_0}, in comparison to that without the thermal-cycling and radiation dilatation $\epsilon_{I_0} = 0$, as shown in Figs. 6, 7 and 8.

(c) The order of magnitude of the neutron flux as well as the total integrated flux distributed in the fuel zone and contained in those terms of $a\alpha$ in Eqs. 7.42, 7.43, 7.44, 7.47 and 7.48 has great effect on the creep stresses and strains developed in the fuel element. The greater the flux is, the higher the creep stresses and strains will be.

(d) The cladding material provides structural strength and corrosion protection for the fuel material under consideration. Therefore, the strength and behavior of the cladding material are the important factors governing the creep strains, Fig. 8, and the mechanical integrity of the fuel element.

(e) While ϵ_{I0} is an important physical strain parameter,

ε_{t_0} is a significant mechanical strain parameter in the creep strain and stress equations derived above. In fact, both ε_{I_0} and ε_{t_0} have very important influence on the physical and mechanical stability of the fuel element. An excessive amount of either strain parameter could cause the fuel element to become unstable in the reactor operation.

(f) It is evident from the creep stress and strain equations derived and the numerical results obtained in the calculation above that a thermoelastic or a non-irradiated inelastic analysis for stress and strain distribution in the fuel elements used for nuclear power reactors is inadequate.

6. Finally, the thermal, radiation creep, the radiation damage and the desired higher operation temperatures and burn-ups of the fuel material pose an important scientific and technological problem in the development of a fuel element that must have physical and mechanical stability for the successful operation, performance and economics in the production of nuclear power.

IX. REFERENCES

1. Thomas, D. E., Fillnow, R. H., Goldman, K. M., Hino, J., Van Thyne, R. J., Holtz, F. C., and McPherson, D. J. Properties of gamma-phase alloy of uranium. International Conference on Peaceful Uses of Atomic Energy, 2nd, Geneva, 1958. Proceedings 5: 610-618. 1958.

2. Leeser, D. O., Rough, F. A. and Bauer, A. A. Radiation stability of fuel elements for the Enrico Fermi Power reactor. International Conference on Peaceful Uses of Atomic Energy, 2nd, Geneva, 1958. Proceedings 5: 587-592. 1958.

3. Cunningham, J. E., Beaver, R. J., Thurber, W. C. and Waugh, R. C. Fuel dispersions in aluminum-base elements for research reactors. U.S. Atomic Energy Commission Report No. TID-7546 [Technical Information Service Extension, AEC]. 1957.

4. Weber, C. E. and Hirsch, H. H. Metallurgy and fuels. Progress in Nuclear Energy, Series 5, 1: 525. Pergamon Press, Limited, London. 1956.

5. Hayward, B. R. and Bentle, G. G. Effect of burn-up on metallic fuel elements operating at elevated temperature. International Conference on Peaceful Uses of Atomic Energy, 2nd, Geneva, 1958. Proceedings 5: 537-542. 1958.

6. Paine, S. H. and Kittel, J. H. Irradiation effects in uranium and its alloys. International Conference on Peaceful Uses of Atomic Energy, 1st, Geneva, 1955. Proceedings 7: 445-454. 1955.

7. Pugh, S. F. Damage occurring in uranium during burn-up. International Conference on Peaceful Uses of Atomic Energy, 2nd, Geneva, 1958. Proceedings 5: 441-444. 1958.

8. Hardy, H. K. and Lawton, H. The assessment and testing of fuel elements. International Conference on Peaceful Uses of Atomic Energy, 2nd, Geneva, 1958. Proceedings 5: 521-531. 1958.

9. Roberts, A. C. Thermal cycling creep of alpha uranium. Acta Metallurgica 8: 817-819. 1960.

10. Chiswick, H. H. and Kelman, L. R. Thermal cycling effects in uranium. International Conference on Peaceful Uses of Atomic Energy, 1st, Geneva, 1955. Proceedings 9: 147-158. 1955.

11. Burke, J. E. and Turkalo, A. M. Deformation of zinc bicrystals by thermal ratcheting. Transaction, American Institute of Mining and Metallurgical Engineers 194: 651-656. 1952.

12. Konobeevsky, S. T., Pravadyuk, N. F. and Kutaitsev, V. I. Effects of irradiation on structure and properties of fissionable materials. International Conference on Peaceful Uses of Atomic Energy, 1st, Geneva, 1955. Proceedings 7: 433-440. 1955.

13. Roberts, A. C. and Cattrell, A. H. Creep of alpha-uranium during irradiation with neutrons. Philosophical Magazine Series 8, 1: 711-717. 1956.

14. Zaimovsky, A. S., Sergeev, G. Y., Titova, V. V., Levitsky, B. M. and Sokursky, Y. N. Influence of the structure and properties of uranium on its behavior under irradiation. International Conference on Peaceful Uses of Atomic Energy, 2nd, Geneva, 1958. Proceedings 5: 566-673. 1958.

15. Weber, C. E. Radiation damage in non-metallic fuel elements. International Conference on Peaceful Uses of Atomic Energy, 2nd, Geneva, 1958. Proceedings 5: 619-627. 1958.

16. Glasstone, S. and Edlund, M. C. The elements of nuclear reactor theory. D. Van Nostrand, Inc., Princeton, N. J. 1952.

17. Karman, T. V. and Biot, A. M. Mathematical methods in engineering. McGraw-Hill Book Co., Inc., New York, N. Y. 1940.

18. Roberts, L. D., Hill, J. E. and McGammon, G. A study of the slowing down distribution of Sb^{124}-Be photo neutrons in graphite and the use of In foils. U.S. Atomic Energy Commission Report No. ORNL-201 [Oak Ridge National Lab., Tenn.]. 1950.

19. Reinke, C. F., Neimark, R. and Kittel, J. H. Metallurgical evaluation of failed borax-IV reactor fuel elements. U.S. Atomic Energy Commission Report No. ANL-6083 [Argonne National Laboratory, Argonne, Illinois]. May, 1961.

20. Merckx, K. R. Mechanical models for tubular reactor fuel elements. ASME Paper No. 61-WA-198 [The American Society of Mechanical Engineers]. 1962.

21. Mises, R. V. Mechanik der festen Koerper in plastisch deformablen Zustand. Goettinger Nachrichten, Mathematisch-Physikalische Klasse 1913: 582-592. 1913.

22. Ma, B. M. Creep analysis of rotating solid disks with variable thickness and temperature. Journal of the Franklin Institute 271: 40-55. 1961.

23. Shober, F. R., Marsh, L. L. and Manning, G. K. The mechanical properties of beta-quenched uranium at elevated temperatures. U.S. Atomic Energy Commission Report No. BMI-1036 [Battelle Memorial Institute, Columbus, Ohio]. 1955.

24. Merckx, K. R. A model of mechanical behavior evaluated with creep tests applied to alpha uranium. U.S. Atomic Energy Commission Report No. HW-40494 [Hanform Laboratories, Richland, Wash.]. 1955.

25. Barnes, R. S., Churchman, A. T., Curtis, G. C., Eldred, V. W., Enderby, J. A., Foreman, A. J. E., Plail, O. S., Pugh, S. F., Walton, G. N. and Wyatt, L. M. Swelling and inert gas diffusion in irradiated uranium. International Conference on Peaceful Uses of Atomic Energy, 2nd, Geneva, 1958. Proceedings 5: 543-565. 1958.

26. Hardy, H. K. and Lawton, H. The assessment and testing of fuel elements. International Conference on Peaceful Uses of Atomic Energy, 2nd, Geneva, 1958. Proceedings 5: 521-531. 1958.

27. Nadai, A. The influence of time upon creep the hyperbolic sine creep law. In Stephen Timoshenko Anniversary Volume. pp. 155-165. Macmillan Co., New York, N. Y. 1938.

28. Hill, R. The mathematical theory of plasticity. Oxford Press, Oxford, England. 1950.

29. Reactor handbook. Vol. 4: Materials. U.S. Atomic Energy Commission Report No. AECD-3645: 391 [Technical Information Service Extension, AEC]. 1955.

30. Kemper, R. S. and Zimmerman, D. L. Neutron irradiation effects on the tensile properties of Zircaloy-2. U.S. Atomic Energy Commission Report No. HW-52323 [Hanford Laboratories, Richland, Wash.]. 1957.

31. Pankaskie, P. J. Creep properties of Zircaloy-2 for design application. U.S. Atomic Energy Commission Report No. HW-75267 [Hanford Laboratories, Richland, Wash.]. 1962.

32. Holden, A. N. Physical metallurgy of uranium. Addison-Wesley Publishing Co., Inc., Reading, Mass. 1958.

X. ACKNOWLEDGEMENT

The author wishes to express his deep gratitude to Dr. Glenn Murphy, Distinguished Professor and Head of the Department of Nuclear Engineering, for his guidance, encouragement and generous advice in the preparation of this work.

XI. APPENDIX A: THE SOLUTIONS FOR NEUTRON FLUX DISTRIBUTION

The basic neutron diffusion equations for the lattice cell in the cylindrical coordinate system are given by

$$\frac{d^2\phi_0}{dr^2} + \frac{1}{r}\frac{d\phi_0}{dr} - \kappa_0^2\phi_0 = 0 \qquad r_i \le r \le r_0 \qquad (4.1b)$$

$$\frac{d^2\phi_1}{dr^2} + \frac{1}{r}\frac{d\phi_1}{dr} - \kappa_1^2\phi_1 + q_1/D_1 = 0 \qquad 0 \le r \le r_i \qquad (4.2b)$$

$$\frac{d^2\phi}{dr^2} + \frac{1}{r}\frac{d\phi_2}{dr} - \kappa_2^2\phi_2 + q_2/D_2 = 0 \qquad r_0 \le r \le r_1 \qquad (4.3b)$$

The general solution for Eq. 4.1b is given by

$$\phi_0 = C_1 I_0(\kappa_0 r) + C_2 K_0(\kappa_0 r) \qquad (a)$$

For Eqs. 4.2b and 4.3b the complementary solutions of the homogeneous parts and the particular solutions of the inhomogeneous parts are, respectively, given by

$$\phi_{1_c} = C_3 I_0(\kappa_1 r) + C_4 K_0(\kappa_1 r) \qquad \phi_{1_p} = q_1/\Sigma_{a_1}$$

$$\phi_2 = C_5 I_0(\kappa_2 r) + C_6 K_0(\kappa_2 r) \qquad \phi_{2_p} = q_2/\Sigma_{a_2}$$

Hence, the complete solutions for Eqs. 4.2b and 4.3b are

$$\phi_1 = C_3 I_0(\kappa_1 r) + C_4 K_0(\kappa_1 r) + q_1/\Sigma_{a_1} \qquad 0 \le r \le r_i \qquad (b)$$

$$\phi_2 = C_5 I_0(\varkappa_2 r) + C_6 K_0(\varkappa_2 r) + q_2/\Sigma_{a_2} \qquad r_0 \leq r \leq r_1 \quad (c)$$

where

$I_0(\varkappa_0 r)$, $I_0(\varkappa_1 r)$, $I_0(\varkappa_2 r)$ ≡ the modified Bessel functions of the first kind of the zero order

$K_0(\varkappa_0 r)$, $K_0(\varkappa_1 r)$, $K_0(\varkappa_2 r)$ ≡ the modified Bessel functions of the second kind of the zero order

$C_1, C_2, \cdots, C_6$ = integration constants

Of the problem the boundary conditions used to determine these integration constants are as follows:

The required, physical condition

$$\phi_0 = \text{finite value} \quad \text{for} \quad r = 0 \qquad (d)$$

The continuity conditions of neutron flux on the interfaces

$$\phi_0 = \phi_1 \qquad \text{at} \qquad r = r_i \qquad (e)$$

$$\phi_0 = \phi_2 \qquad \text{at} \qquad r = r_0 \qquad (f)$$

The continuity conditions of neutron current on the interfaces

$$D_0 \frac{d\phi_0}{dr} = D_1 \frac{d\phi_1}{dr} \qquad \text{at} \qquad r = r_i \qquad (g)$$

$$D_0 \frac{d\phi_0}{dr} = D_2 \frac{d\phi_2}{dr} \qquad \text{at} \qquad r = r_0 \qquad (h)$$

The condition that there is no net flow of neutron current at the outside boundary of the lattice cell

$$\frac{d\phi_2}{dr} = 0 \qquad \text{for} \qquad r = r_1 \qquad (i)$$

From (b) and (d), when $r = 0$, $K_0(\varkappa_1 r) = \infty$, it is necessary to take $C_4 = 0$ so that

$$\phi_1 = C_3 I_0(\varkappa_1 r) + q_1/\Sigma_{a_1} \qquad 0 \leq r \leq r_i \tag{4.4}$$

From (c) and (i) at $r = r_1$, it gives

$$(d\phi_2/dr)_{r=r_1} = \varkappa_2 \left[C_5 I_1(\varkappa_2 r_1) - C_6 K_1(\varkappa_2 r_1) \right] = 0$$

$$C_5 = C_6 K_1(\varkappa_2 r_1)/I_1(\varkappa_2 r_1) \tag{j}$$

hence

$$\phi_2 = \frac{C_6}{I_1(\varkappa_2 r_1)} \left[K_1(\varkappa_2 r_1) I_1(\varkappa_0 r) + I_1(\varkappa_2 r_1) K_0(\varkappa_2 r) \right] + \frac{q_2}{\Sigma_{a_2}}$$

$$r_0 \leq r \leq r_1 \tag{4.5}$$

From (a), (e) and Eq. 4.4, it follows that

$$C_1 I_0(\varkappa_0 r_i) + C_2 K_0(\varkappa_0 r_i) = C_3 I_0(\varkappa_1 r_i) + q_1/\Sigma_{a_1}$$

or

$$C_3 = \left[C_1 I_0(\varkappa_0 r_i) + C_2 K_0(\varkappa_0 r_i) - \frac{q_1}{\Sigma_{a_1}} \right] / I_0(\varkappa_1 r_i) \tag{k}$$

From (a), (g) and Eq. 4.4, it also gives

$$D_0 \varkappa_0 \left[C_1 I_1(\varkappa_0 r_i) - C_2 K_1(\varkappa_0 r_i) \right] = D_1 \varkappa_1 C_3 I_1(\varkappa_1 r_i)$$

so

$$C_3 = D_0 \varkappa_0 \left[C_1 I_1(\varkappa_0 r_i) - C_2 K_1(\varkappa_0 r_i) \right] / D_1 \varkappa_1 I_1(\varkappa_1 r_i) \tag{ℓ}$$

From (k) and (ℓ), C_3 is eliminated. Thus

$$C_1\left[I_0(\varkappa_0 r_i) I_1(\varkappa_1 r_i) - \frac{D_0\varkappa_0}{D_1\varkappa_1} I_0(\varkappa_0 r_i) I_0(\varkappa_1 r_i) \right] = \frac{q_1}{\Sigma_{a_1}} I_1(\varkappa_0 r_i)$$

$$- C_2\left[I_1(\varkappa_1 r_i) K_0(\varkappa_0 r_i) + \frac{D_0\varkappa_0}{D_1\varkappa_1} I_0(\varkappa_1 r_i) K_1(\varkappa_0 r_i) \right]$$

or

$$C_1 = G\, q_1/\Sigma_{a_1} - C_2 H \qquad (m)$$

where

$$G = I_1(\varkappa_0 r_i)/\left[I_0(\varkappa_0 r_i) I_1(\varkappa_1 r_i)\left(1 - \frac{D_0\varkappa_0}{D_1\varkappa_1}\right) \right] \qquad (n)$$

$$H = \frac{I_1(\varkappa_1 r_i) K_0(\varkappa_0 r_i) + \frac{D_0\varkappa_0}{D_1\varkappa_1} I_0(\varkappa_1 r_i) K_1(\varkappa_0 r_i)}{I_0(\varkappa_0 r_i) I_1(\varkappa_1 r_i) - \frac{D_0\varkappa_0}{D_1\varkappa_1} I_0(\varkappa_0 r_i) I_0(\varkappa_1 r_i)}$$

$I_1(\varkappa_0 r_i)$, $I_1(\varkappa_1 r_i)$, $I_1(\varkappa_2 r_1)$ ≡ the modified Bessel functions of the first kind of the first order

$K_1(\varkappa_0 r_i)$, $K_1(\varkappa_1 r_i)$, $K_1(\varkappa_2 r_1)$ ≡ the modified Bessel functions of the second kind of the first order

By substituting (m) into (a), it yields

$$\phi_0 = G \frac{q_1}{\Sigma_{a_1}} I_0(\varkappa_0 r) - C_2\left[H I_0(\varkappa_0 r) - K_0(\varkappa_0 r) \right] \qquad (4.6)$$

$$0 \leq r \leq r_i$$

By introducing Eqs. 4.5 and 4.6 into (f) and (h) respec-

tively, it can be checked that

$$\phi_2 = \frac{C_6}{I_1(\varkappa_2 r_1)}\left[K_1(\varkappa_2 r_1) I_1(\varkappa_2 r) + I_1(\varkappa_2 r_1) K_0(\varkappa_2 r) \right] + \frac{q_2}{\Sigma_{a_2}}$$

$$r_0 \leq r \leq r_1 \qquad (4.5)$$

for the neutron flux; and it also determines the constants below:

$$C_6 = \frac{D_0 \varkappa_0 \left[G I_1(\varkappa_0 r_0) - C_2 \{ H I_1(\varkappa_0 r_0) + K_1(\varkappa_0 r_0) \} \right] I_1(\varkappa_2 r_1)}{D_2 \varkappa_2 \qquad K_1(\varkappa_2 r_1) I_0(\varkappa_2 r_0) - I_1(\varkappa_2 r_1) K_1(\varkappa_2 r_0)} \qquad (o)$$

$$C_2 = \frac{G\left[I_0(\varkappa_0 r_0) - I_1(\varkappa_0 r_0)\, J \right] + q_2/\Sigma_{a_2}}{H\left[I_0(\varkappa_0 r_0) - I_1(\varkappa_0 r_0)\, J \right] - \left[K_0(\varkappa_0 r_0) + K_1(\varkappa_0 r_0)\, J \right]} \qquad (p)$$

where

$$J = \frac{D_0 \varkappa_0 \left[K_1(\varkappa_2 r_1) I_0(\varkappa_2 r_0) + I_1(\varkappa_2 r_1) K_1(\varkappa_2 r_0) \right]}{D_2 \varkappa_2 \left[K_1(\varkappa_2 r_1) I_0(\varkappa_2 r_0) - I_1(\varkappa_2 r_1) K_1(\varkappa_2 r_0) \right]} \qquad (q)$$

XII. APPENDIX B: RESULTS OF THE CALCULATION

By using Eqs. 6.24, 7.11a, 7.14a, 7.15a and 7.16a

$$\theta = \theta_{r_i} + \frac{a\beta}{2k} M_1 \ln \frac{x}{x_i} - \frac{a}{2k}\Big[(1 + br_0^2c^2)\left(\frac{x^2}{2} - x_i^2 \ln \frac{x}{x_i}\right) + br_0^2\{x^3\left(\frac{x}{8} - \frac{4c}{9}\right) - x_i^3\left(\frac{x_i}{2} - \frac{4c}{3}\right)\ln \frac{x}{x_i}\} - M_2 \Big] \tag{6.24}$$

$$\epsilon_R = \alpha\,\theta + \epsilon_I \tag{7.11a}$$

$$\epsilon_t = \frac{1}{x^2}\Big[\epsilon_{t_0} - 3\int_x^1 \epsilon_R x dx \Big] \qquad x_i \le x \le 1 \tag{7.14a}$$

$$\epsilon_r = \frac{1}{x^2}\Big[- \epsilon_{t_0} + 3\int_x^1 \epsilon_R x dx - 3x \frac{\partial}{\partial x} \int_x^1 \epsilon_R x dx \Big] \qquad x_i \le x \le 1 \tag{7.15a}$$

$$\epsilon = \frac{1}{2}(\epsilon_r - \epsilon_t)$$

$$= \frac{1}{x^2}\Big[- \epsilon_{t_0} + 3\int_x^1 \epsilon_R x dx - \frac{3x}{2} \frac{\partial}{\partial x} \int_x^1 \epsilon_R x dx \Big] \qquad x_i \le x \le 1 \tag{7.16a}$$

and integrating between the limits $x = 1$ and any point x within the fuel zone, Eqs. 7.42, 7.43 and 7.44 for the components of creep strain, ϵ_t, ϵ_r and ϵ are obtained. Further, by using Eqs. 6.4a, 6.22, 6.24, the first of Eqs. 7.23, the

second of Eqs. 7.26 and Eq. 7.41

$$\theta = \theta_{r_i} + \frac{\beta}{k} \ln \frac{r}{r_i} \int_{r_i}^{r_0} q_v r dr - \frac{1}{k} \int_{r_i}^{r} \frac{1}{r} \int_{r_i}^{r} q_v r dr dr$$

$$= \theta_{r_i} + \frac{\beta r_0^2}{k} \ln \frac{x}{x_i} \int_{x_i}^{1} q_v x dx - \frac{r_0^2}{k} \int_{x_i}^{x} \frac{1}{x} \int_{x_i}^{x} q_v x dx dx$$

$$x_i \leq x \leq 1 \qquad (6.4a)$$

$$q_v = a\left[1 + br_0^2(x - c)^2\right] \qquad (6.22)$$

$$\epsilon = \lambda s \qquad (7.23a)$$

$$\sigma_r = \sigma_{r_i} - 2\int_{x_i}^{x} \frac{s dx}{x} \qquad x_i \leq x \leq 1 \qquad (7.26a)$$

$$\epsilon_I = \epsilon_{I_0} e^{|x - x_m|} \qquad (7.41)$$

Eqs. 7.47 and 7.48 for ϵ_R and σ_r are respectively found after σ_{t_c} has been determined from Eqs. 7.36 and 7.39 and σ_{r_i} determined from Eq. 7.32.

Finally, with the aid of the last of Eqs. 7.22, the components of stress σ_t and σ_z can be obtained from Eqs. 7.28 and 7.29 respectively.

$$-\epsilon_R = \lambda s_z \qquad (7.22a)$$

$$\sigma_t = \sigma_r - 2s \qquad (7.28)$$

$$\sigma_z = \frac{3}{2} s_z - s + \sigma_{r_i} \qquad (7.29)$$

With the data given for the example, the results calculated from these equations are tabulated below.

Table 1. Tangential strain ϵ_t

(a) $\phi = 5\ (10^{11})$ neutrons/cm^2-sec at outer radius r_0 of fuel zone
$= \phi_{max}$
$\theta_{r_i} = 550°F$, $\epsilon_{t_0} = 0.03$, $\epsilon_{I_0} = 0.005$

x	ϵ_t β=0.50 (10^{-3})	ϵ_t β=0.40 (10^{-3})	ϵ_t β=0.30 (10^{-3})	$\epsilon_t/\epsilon_{t_0}$ β=0.50	$\epsilon_t/\epsilon_{t_0}$ β=0.40	$\epsilon_t/\epsilon_{t_0}$ β=0.30
0.6	-5.68	3.40	12.47	-0.189	0.113	0.416
0.7	10.36	16.61	22.86	0.345	0.554	0.762
0.8	20.37	24.29	27.14	0.679	0.810	0.905
0.9	25.66	27.51	29.35	0.855	0.917	0.978
1.0	30.00	30.00	30.00	1.000	1.000	1.000

Table 1 (Continued).

(b) ϕ = 5 (10^{10}) neutrons/cm^2-sec at r_o

θ_{r_i} = 550°F, ϵ_{t_o} = 0.03, β = 0.50

x	ϵ_t $\epsilon_{I_o}=0$ (10^{-3})	ϵ_t $\epsilon_{I_o}=0.005$ (10^{-3})	ϵ_t $\epsilon_{I_o}=0.01$ (10^{-3})	$\epsilon_t/\epsilon_{t_o}$ $\epsilon_{I_o}=0$	$\epsilon_t/\epsilon_{t_o}$ $\epsilon_{I_o}=0.005$	$\epsilon_t/\epsilon_{t_o}$ $\epsilon_{I_o}=0.01$
0.6	62.66	42.30	21.94	2.089	1.310	0.731
0.7	48.91	38.76	28.61	1.630	1.292	0.954
0.8	40.15	35.46	30.77	1.338	1.182	1.026
0.9	34.24	32.19	30.14	1.141	1.073	1.005
1.0	30.00	30.00	30.00	1.000	1.000	1.000

(c) ϕ = 5 (10^{11}) neutrons/cm^2-sec at r_o

ϵ_{t_o}=0.03, β = 0.50, ϵ_{I_o} = 0.005

x	ϵ_t $\theta_{r_i}=450°F$ (10^{-3})	ϵ_t $\theta_{r_i}=550°F$ (10^{-3})	ϵ_t $\theta_{r_i}=650°F$ (10^{-3})	$\epsilon_t/\epsilon_{t_o}$ $\theta_{r_i}=450°F$	$\epsilon_t/\epsilon_{t_o}$ $\theta_{r_i}=550°F$	$\epsilon_t/\epsilon_{t_o}$ $\theta_{r_i}=650°F$
0.6	-2.48	-5.68	-8.88	-0.083	-0.189	-0.296
0.7	+11.65	+10.36	+9.07	+0.388	+0.345	+0.302
0.8	+21.39	+20.37	+19.35	+0.713	+0.679	+0.645
0.9	+26.08	+25.66	+25.24	+0.869	+0.855	+0.841
1.0	+30.00	+30.00	+30.00	+1.000	+1.000	+1.000

Table 2. Radial strain ϵ_r

(a) $\phi = 5\ (10^{10})$ neutrons/cm^2-sec at r_o

$\theta_{r_i} = 550°F$, $\beta = 0.50$, $\epsilon_{I_o} = 0.005$

x	ϵ_r $\epsilon_{t_o}=0.005$ (10^{-3})	ϵ_r $\epsilon_{t_o}=0.01$ (10^{-3})	ϵ_r $\epsilon_{t_o}=0.02$ (10^{-3})	ϵ_r $\epsilon_{t_o}=0.03$ (10^{-3})
0.6	71.57	57.68	29.90	2.12
0.7	79.79	69.59	49.19	28.78
0.8	94.93	87.12	71.49	55.86
0.9	108.40	102.23	89.88	77.53
1.0	97.66	97.66	82.66	72.66

(b) $\phi = 5\ (10^{10})$ neutrons/cm^2-sec at r_o

$\theta_{r_i} = 550°F$, $\beta = 0.50$, $\epsilon_{I_o} = 0$

x	ϵ_r $\epsilon_{t_o}=0.005$ (10^{-3})	ϵ_r $\epsilon_{t_o}=0.02$ (10^{-3})	ϵ_r $\epsilon_{t_o}=0.03$ (10^{-3})
0.6	32.89	-8.78	-36.56
0.7	53.66	+22.46	+2.05
0.8	72.12	+48.68	+33.05
0.9	89.78	+71.26	+58.91
1.0	79.34	+64.34	+54.34

Table 3. Effective strain ϵ (from Table 1b and Table 2, $\epsilon = \frac{1}{2}(\epsilon_r - \epsilon_t)$)

ϕ = 5 (10^{10}) neutrons/cm^2-sec at r_0

θ_{r_i} = 550°F, β = 0.50, ϵ_{t_0} = 0.03

x	ϵ $\epsilon_{I_0}=0$ (10^{-3})	ϵ $\epsilon_{I_0}=0.005$ (10^{-3})	ϵ $\epsilon_{I_0}=0.01$ (10^{-3})
0.6	-49.61	3.90	33.42
0.7	-23.43	9.21	27.68
0.8	-3.55	17.75	38.89
0.9	+12.34	25.94	37.29
1.0	+12.17	21.33	30.49

Table 4. Resultant linear thermal and radiation dilatation ϵ_R

ϕ = 5 (10^{10}) neutrons/cm^2-sec at r_0

θ_{r_i} = 550°F, β = 0.50

x	ϵ_R $\epsilon_{I_0}=0$ (10^{-3})	ϵ_R $\epsilon_{I_0}=0.005$ (10^{-3})	ϵ_R $\epsilon_{I_0}=0.01$ (10^{-3})
0.6	6.60	12.70	18.80
0.7	7.37	12.89	18.41
0.8	7.92	12.92	17.92
0.9	8.10	12.62	19.14
1.0	7.88	13.98	20.08

Table 5. The parameter λ, $(psi)^{-1}$

$\phi = 5\ (10^{10})$ neutrons/cm^2-sec at r_0

$\theta_{r_i} = 550°F$, $\beta = 0.50$, $\epsilon_{t_0} = 0.03$

$\sigma_{t_c} = 20{,}000$ psi, $J_{2_c} = 17{,}500$ psi, $\mu = 3.33\ (10^{-6})\ (psi)^{-1}$

$J_2 = 3{,}000$ psi, $\sigma_{r_i} = -1{,}000$ psi

x	λ $\epsilon_{I_0}=0$ (10^{-5})	λ $\epsilon_{I_0}=0.005$ (10^{-5})	λ $\epsilon_{I_0}=0.01$ (10^{-5})
0.6	3.6327	2.5230	1.5773
0.7	2.8473	2.3280	1.8913
0.8	2.3520	2.1467	1.9890
0.9	2.0167	1.9873	1.9860
1.0	1.7760	1.8660	1.8280

Table 6. Radial, tangential and axial stresses

ϕ = 5 (10^{10}) neutrons/cm^2-sec at r_o

θ_{r_i} = 550°F, β = 0.50, ϵ_{t_o} = 0.03, σ_{r_i} = -1,000 psi

x	σ_r/σ_{r_i}	σ_t/σ_{r_i}	σ_z/σ_{r_i}
	ϵ_{I_o}=0	ϵ_{I_o}=0	ϵ_{I_o}=0
0.6	-1.000	-4.450	-2.998
0.7	-0.177	-3.613	-2.282
0.8	+0.971	-2.443	-1.242
0.9	+2.210	-1.186	-0.091
1.0	+3.678	+0.300	+1.323

x	σ_r/σ_{r_i}	σ_t/σ_{r_i}	σ_z/σ_{r_i}
	ϵ_{I_o}=0.005	ϵ_{I_o}=0.005	ϵ_{I_o}=0.005
0.6	-1.000	-4.354	-3.432
0.7	-0.169	-3.499	-2.665
0.8	+0.742	-2.562	-1.813
0.9	+1.674	-1.566	-0.974
1.0	+2.721	-0.495	-0.011

x	σ_r/σ_{r_i}	σ_t/σ_{r_i}	σ_z/σ_{r_i}
	ϵ_{I_o}=0.01	ϵ_{I_o}=0.01	ϵ_{I_o}=0.01
0.6	-1.000	-3.782	-4.179
0.7	-0.322	-3.348	-3.295
0.8	+0.430	-2.664	-2.468
0.9	+1.142	-1.944	-1.852
1.0	+2.052	-1.230	-1.246